# BALANCE CONTROL FOR A STANDING BIPED AND STABILITY ANALYSIS USING THE CONCEPT OF LYAPUNOV EXPONENTS

By

XIANGPENG WANG

A Thesis

Submitted to the Faculty of Graduate Studies

in Partial Fulfillment of the Requirement

for the Degree of

MASTER OF SCIENCE

Department of Mechanical and Manufacturing Engineering

The University of Manitoba

Winnipeg, Manitoba, Canada

THE UNIVERSITY OF MANITOBA

FACULTY OF GRADUATE STUDIES

*****

COPYRIGHT PERMISSION

# BALANCE CONTROL FOR A STANDING BIPED AND STABILITY ANALYSIS USING THE CONCEPT OF LYAPUNOV EXPONENTS

BY

XIANGPENG WANG

A Thesis/Practicum submitted to the Faculty of Graduate Studies of The University of Manitoba in partial fulfillment of the requirement of the degree

MASTER OF SCIENCE

# Table of Contents

# Abstract

The mechanics of balance control essential in biped locomotion has attracted much attention in the past two decades. There are three requirements in designing balance controllers: (1) maintaining the postural stability, (2) improving the energy efficiency of the control systems and (3) satisfying the constraints between the foot-link and the ground.

In spite of the attempts, there has been little success in developing balance controllers which satisfy all three requirements. The lack of a constructive tool for stability analysis is one of the obstacles. Stability analysis based on Lyapunov's stability theory is challenging, due both to the complexity of the system and to its inflexibility to include optimization criterion. It has often been assumed that the constraints between the feet and the ground are always satisfied once the feet contact the ground. However, such constraints have significant effect on control design.

This thesis is concerned with biped balancing in the upright standing posture and the stability analysis of the control systems. The work has been carried out with two objectives: (1) design optimal controllers which can satisfy the constraints between the foot-link and the ground while minimizing the energy cost, and (2) perform stability analysis of the proposed systems using the concept of Lyapunov exponents.

The biped robot is simplified as two inverted pendulums, representing the legs and the trunk. The feet are modeled as a separate link, stationary on level ground. Two optimal controllers are proposed in this thesis. A LQR balance control is first designed to optimize the total energy consumption of torque outputs. A GA-based PD balance control is then proposed to satisfy the constraints between the foot-link and the ground; as well as minimize the energy consumption of torque outputs. The effectiveness of the control laws are tested through computer simulations. Note that, the constraints between the foot-link and the ground are not considered in the design of LQR controller, but their satisfaction is tested through simulations.

Since the biped upright posture is inherently unstable, stability analysis of the control systems is required. The concept of Lyapunov exponents is a powerful tool when analyzing the stability of dynamic systems. However, for complex or unknown systems, deriving system Jacobians is extremely difficult.

A novel approach based on neural networks has been proposed for Jacobian derivation. Neural networks are used to identify the system dynamics, and then numerical Jacobians are derived from the neural model for the calculation of Lyapunov exponents. To increase the modeling accuracy of the biped balance system, Radial Basis Function neural networks (RBFNNs) are employed, providing a capability for nonlinear system identification.

The work contributes significantly to the stability analysis of practical complex or unknown engineering systems in that, a reliable and constructive method for calculating Lyapunov exponents based on neural network identification has been developed.

# Acknowledgements

I would like to express my heart-felt gratitude to my advisor, Dr. Christine Q. Wu for providing me the necessary guidance and inspiration to carry out this work. She allowed me the freedom to develop my ideas, yet she was always there to help me whenever I needed the support.

I sincerely thank Dr. Caixia Yang for her constructive suggestions. I am grateful to her for patiently answering all my queries regarding the Lyapunov exponents and classical mechanics.

I would also like to express my gratitude to Dr. Reza Ghorbani for enhancing my understanding of neural networks and Genetic Algorithms.

A special word of thanks is due to my colleague Yan Lu who was always available for discussions and suggestions.

Finally, I would like to acknowledge my heart-felt gratitude to my mother for her long-term support and understanding.

To My Mother

# List of Figures

# List of Tables

# Chapter 1

# Introduction

## 1.1 Motivations

Biped robots have significant advantages over conventional wheeled robots because their mechanical design allows for better mobility. Dynamic control and the ability to lift a supporting point off the ground give legged robots the ability to move over rough terrain and negotiate obstacles more easily than wheeled robots. However, along with the advantage of increased mobility, comes the challenging problems of balance control and stability which need to be addressed through advanced design and analysis.

Maintenance of a standing biped at the upright posture is a key requirement for safe and successful co-existence of biped robots within normal human environments. Since only the feet are in contact with the ground, a standing biped is always subjected to constraints (Yang and Wu 2006), i.e., the ground reaction force being upward (the gravity constraint), friction between the feet and the ground being lower than the maximum friction (the friction constraint) and the pressure center being within the contact surface between the feet and the ground (the center of pressure constraint). Much of previous research on

balance control has been carried out under the assumption that all these constraints are satisfied. This assumption although simplifying the problem, can be misleading.

Limited previous research on biped balance control considered the constraints between the foot-link and the ground. However, these balance systems are not energy-efficient. Since biped robots need to carry their energy sources, a lower rate of energy consumption would directly contribute to a longer work cycle. Energy efficiency is an important issue to be resolved before the use of bipeds is viable. The design of energy-efficient control algorithms with the satisfaction of the above constraints for biped standing is a challenge.

Another challenge in biped design is the stability analysis of control systems. Since the upright posture of the standing biped is inherently unstable, control methods have to be very effective and safety aspects are mandatory, *i.e.*, any falls are liable to result in a fatal failure. The stability of the control systems needs be analyzed to determine the stability region. Due to the complexity of the biped dynamics and control laws, the use of classical stability analysis tools is extremely difficult. For example, Lyapunov's second method is widely used, but it is difficult to derive Lyapunov functions for complex biped models. Alternatively, Lyapunov exponents, defined as the average exponential rates of divergence or convergence of nearby trajectories in the state space, can characterize the system's stability. The calculation of Lyapunov exponents is based on system Jacobians derived from mathematical models. Though the concept of Lyapunov exponents is an effective stability analysis tool for biped control, it has not been widely used. One of the reasons is the difficulty in deriving Jacobian matrices. For unknown systems it is impossible to

determine Jacobians. Even if the models are obtained, it requires enormous work to derive Jacobian from complex dynamics. Thus, a new approach to derive Jacobians from complex or unknown systems should be developed for the stability analysis using the concept of Lyapunov exponents.

## 1.2 Literature Review

### 1.2.1 Biped Dynamic Models

Biped robots are expected as a rational form of machines to act in the environment that humans live, and to support people through interactions. In order to maintain biped balance during standing and locomotion, the posture and motion should be generated in real-time in accordance with the dynamics. This requires a large amount of computation and has not been implemented to date. Therefore, biped robots should be modeled into simple forms, which are easier to implement.

Kajita *et al.* (2001) introduced the three-dimensional inverted model for the walking control of a 12-DOF biped robot. The dominant biped dynamics is represented by a single inverted pendulum which connects the supporting foot and the center of mass of the whole robot. The model consists of a concentrated mass at the torso and neglects the mass and the inertial effects of the legs, which extend from the centre of the supporting base to the location of the center of mass of the robot. The model allows for the separate controller design of sagittal and lateral motion, significantly simplifying the analysis of dynamic motion. To extend the basic inverted model, Park and Kim (1998) developed a gravity-compensated inverted pendulum model. This included the predetermined effects

of the dynamics of the free (swing) leg on ZMP (Zero-moment point) by modeling the robot as two separate inverted pendulums. The model assumes that the swing leg consists of mass concentrated at the location of the feet, and that its dynamics are dominated by gravitational acceleration. In this sense, only the static effect of the swinging leg is considered.

Caballero *et al.* (2000) developed a further extension of the above model that was applicable to biped robots. The model represents the robot as an inverted pendulum with two quasi-static coupled pendulums. Using ZMP stability theory, this model was successfully used to generate stable geometric gaits.

The other model is a multiple-masses inverted pendulum model, which consists of one mass representing the torso, and multiple masses modeling the swinging leg. The foot motion of the swinging leg is predefined, and all other trajectories are calculated iteratively.

Li and Kato (1994) considered the model to be composed of two separate moving masses representing the torso and the legs. Motion generation specific to the surface structure of the ground was pre-determined, while the motion of the torso was adapted in real-time to ensure postural stability. For traditional biped robots, the absence of a torso allows the mass distribution to be modeled as a single point mass. Stability is then maintained by relying on the overall motion of both the supporting leg and the swinging leg.

Gerth and Albert (2001) then proposed a model which considered the dynamic effects of the swinging leg. It is a two-link inverted pendulum robot model, with two masses representing the torso and the swinging leg. The complete dynamic effect of the swinging leg is considered for the generation of the torso motion.

Multi-link planar models are used to study biped locomotion and the related properties. Miura and Shimoyama (1984) developed a three-link biped robot to walk sideways, backward and forward, and studied it in both the sagittal and frontal planes. The results served as a basis for choosing the appropriate feedback control gains. Hurmuzlu and Moskowitz's three-link biped model (1987) has an upright trunk with two lower limbs. Miura and Shimoyama's model (1984) has two lower limbs and a link located at the pitch axis. Hurmuzlu's four-link biped model (1987) put one link above Miura's model. Iqbal *et al.* (1993) used a four-link planar model to study the stability and control of a biped system. The model approximates gross human locomotion in the frontal plane.

A general five-link biped is modeled with a torso and two legs, each leg consisting of a thigh and a shank. The study of this model can be found in Hemami *et al.* (1977), Hurmuzlu (1993), Wu and Chan (2002), Ma and Wu (2002), Mu and Wu (2004). Hemami *et al.* (2004) studied dynamics, stability and control of stepping, via a seven-link two-dimensional sagittal biped model. Furusho and Sano (1990) developed a nine-link biped which included the foot structure and was equipped with foot pressure and ankle torque sensors to provide information about the conditions of contact with the floor. Their work contributed toward the realization of smooth three-dimensional walking with the

sole firmly gripping the floor. Abdallah and Goswami (2005) introduced a planar upright robot model which is a single-leg plus head-arms-trunk (HAT) model in the sagittal plane. The model contains four limbs: the feet, shank, thigh, and HAT. These rigid body limbs are inter-connected through three actuated joints: the ankle, knee, and hip. The feet are free to leave the ground but Abdallah and Goswami assumed that friction was sufficient to prevent slip. The robot has four kinematic feet/ground contact states. In the flat feet phase, the feet are flat against the ground. In the toe phase and heel phase the foot pivots around the toe or the heel respectively. In the airborne phase, the feet completely lift off of the ground. The robot has three degrees of freedom (DOF) in the flat feet phase, four DOF in each of both the Toe and Heel phases and six DOF in the airborne phase.

The balance of biped standing is a basic task for other complex motions such as locomotion and running. Studies on upright standing bipeds are commonly simplified as inverted pendulum models, which significantly simplifies the analysis and calculation of dynamic motion. Ito *et al.* (2006) modeled the biped as an inverted pendulum with a supporting foot segment, connected at the ankle joint. The body segment moves only within the sagittal plane. The foot segment contacts the ground with two points (heel and toe). The foot segment does not slip on the ground and its shape is symmetrical in the anterior-posterior direction. The ankle joint is located in the middle of the foot segment with zero height. Pai and Patton (1997) simplified the biped as an inverted pendulum with a triangular foot-link. The foot position is assumed to be bilaterally symmetric and stationary, and the body link moves in the sagittal plane.

Based on this model, Yang and Wu (2006a) investigated the effect of the constraints, between the feet and the ground on the control design of biped standing. Although these inverted pendulum models simplify analysis, there are resultant performance limitations. The assumption that the model used only the ankle joint to balance the biped is valid when the disturbance is low. Jiang *et al.* (2006) found the ankle and the lumbosacral swayed in approximately the same amplitude during the static upright stance of humans, from the experiment data. They modeled the human body as a two link inverted pendulum system, and proved that this model was reasonable and useful for studying the balance of biped standing.

In this work, the biped is modeled as a two link inverted pendulum presenting the torso and legs with a foot-link, which is adequate for studying various fundamental theoretical problems related to biped standing.

### 1.2.2 Biped Balance Control

Biped balance control is a key development in the area of biped robots and has attracted much attention in the past two decades. Various control strategies such as adaptive control (Hu *et al.* 1999, Chew and Pratt 2001), sliding mode control (Mu and Wu 2004), fuzzy control (Meng and Zhou 2003, Cuevas *et al.* 2005) and neural network control (Kun, A. and Miller 1996, Scesa *et al.* 2005) have been developed.

In considering stability conditions and balance control in biped locomotion (standing, walking and running), several dynamic-based criteria have been defined. The criteria most commonly used are the centre of pressure (COP) criterion (Murray *et al.* 1967),

zero-moment-point (ZMP) criterion (Vukobratović *et al.* 1970) and the Feet Rotation Indicator (FRI) criterion (Goswami 1999). The COP is a point between the feet and the ground on the contact surface where the net ground reaction force actually acts. The FRI is a point on the feet/ground surface, inside or outside the support polygon, where the net ground reaction force would have to act to keep the feet stationary. The support polygon of the biped is defined as the area of physical interaction between the biped and the ground surface. During the single-support phase, it is the area of the supporting foot. During the double-support phase it is defined as the polygon created by the boundary of the two feet. The ZMP is defined as the point on the feet/ground contact surface where, the total forces and moments acting on the robot are zero (Vukobratovic et al. 1970). If ideal conditions are considered whereby neither the feet nor ground can deform under the load and the ground is level, the COP and ZMP locations will always coincide. ZMP is widely used in the study of biped walking.

Park and Rhee (1998) presented a ZMP trajectory control scheme which was determined using fuzzy logic on the leg trajectories. The trunk and swing leg motions were compensated to stabilize the locomotion. Fukuda *et al.* (1997) used touch sensors on the feet of the robot to obtain the actual ZMP trajectory. The joint motion was then determined using recurrent neural networks with the constraint that the ZMP could move out of the support polygon.

Balance maintenance during biped standing is essential for biped balance control. Ito *et al.* (2006) proposed a biped stance maintenance method that contains the integral feedback of

the ground reaction forces, which is used to improve the convergence of the posture to the equilibrium upright position. As a result, the biped posture could adaptively change with respect to external forces. Abdallah and Goswami (2005) presented a two-phase control strategy for robust balance maintenance under a force disturbance. The first phase, called the Reflex Phase, is designed to withstand the immediate effect of the force. The second phase is the Recovery Phase where the system is steered back to a statically stable "home" posture.

The standing biped is always subjected to three constraints between the feet and ground, which include the ground reaction force being upward (gravity constraint), friction between the feet and the ground being lower than the maximum friction (friction constraint), no tipping-over about the toe or the heel and the center of pressure being within the feet/feet (COP constraint). However, research on the effects of constraints on biped locomotion is sparse.

One distinguished work is from Yang and Wu (2006a), where gravity constraint, friction constraint and the center of pressure constraint during biped standing have been considered. They investigated the effects of these constraints on balance control and showed such control bounds have significant effects on predicting fall prevention during biped standing. Such bounds make the control design challenging. They also found that angular velocity plays a crucial role in satisfying the constraints. Furthermore, Yang and Wu (2006b) proposed a PD-based switching state feedback control to stabilize the biped at the upright position while satisfying the constraints between the feet and the ground.

The controller is a simple PD control, as the control is within the control bounds; and it takes the value of the control bounds as it approaches the bounds value.

The design of biped balance control should consider reducing energy consumption of control systems. Since biped robots need to carry their energy sources, a lower rate of energy consumption would directly contribute to a longer work cycle. This is an important issue to be resolved before the use of biped robots is practically viable. So, the design of low energy control algorithms is essential. Silva and Tenreiro Machado (1999) analyzed the energy consumption of walking robots by controlling the locomotion variables. Yamasaki *et al.* (2002) developed control algorithms to reduce the energy consumption of humanoid robots.

The linear quadratic regulator (LQR) optimal feedback is one of many tools to improve control performance. A set of optimal feedback gains may be found which minimizes a quadratic index and makes a closed-loop system stable (Lewis 1986, Bryson and Ho 1987). Many applications of LQR have been reported (see Johnson and Grimble (1987) for details) in recent years. Genetic algorithm (GA) is another optimization tool which is often employed in nonlinear problems and multi-objective optimizations. Arakawa and Fukuda (1996) used a GA to generate the natural motion of biped locomotion with energy optimization. Cabodevial *et al.* (1997) designed an optimal gait for a biped robot based on the expansion of the joint trajectories by Fourier's series using a GA. Golubovic and Hu (2003) presented a GA approach to the development of a locomotion gait for Sony quadruped robots. Capi *et al.* (2003), Park and Choi (2004) used GAs to generate the

optimal trajectory for biped walking. Garder *et al.* (2006) combined an incremental approach with GA to generate precise walking patterns. Much of the above work focused on energy consumption of walking robots.

For balance-keeping during biped standing, Ghorbani and Wu (2007) developed a general regression neural network (GRNN) feedback control. The GRNN controller was also designed to minimize an energy-related cost function while satisfying the constraints between the feet and the ground. The optimization has been carried out using the genetic algorithm (GA) and the GRNN was directly trained during an optimization iteration process to provide the closed loop feedback optimal controller.

In my work, both the energy-efficiency and the satisfaction of the constraints between the feet and the ground are considered for the balance control design of standing bipeds.

### 1.2.3 Stability Analysis

Stability analysis investigates the long-term behavior of motion under the influence of disturbance in the initial states. For stable motion, the effects of the disturbance are insignificant, *i.e.*, the disturbed motion stays close to the undisturbed one. In an unstable case, an infinitesimal disturbance causes a considerable change in the motion. The stability of the biped balance control is a crucial issue and requires analysis.

Lyapunov's stability theory is widely used in the stability analysis of nonlinear control systems (Wu *et al.* 1998a, 1998b). Lyapunov (1892) not only introduced the basic definition of stability for nonlinear systems, but also proved many of the fundamental

theorems. The key requirement in proving system stability using Lyapunov's stability theory is to construct a Lyapunov function. Since no constructive rules or suggestions were given in this theory, the construction of a Lyapunov function for a nonlinear system remains a great challenge, which restricts the applications of this theory. In the past forty years, numerous techniques have been proposed to construct Lyapunov functions for special nonlinear systems. Among others, these techniques include the method of analogy with linear systems by Barbasin (1960), the method of integration by parts by Ponzo (1965), and Huaux (1967), the method of system energy by Marino and Nicosia (1983), the integral methods, the scalar-Lyapunov-function method and the intrinsic method by Chin (1986, 1987, 1988 and 1989) and the extended integral method by Wu (Wu 1996 and references cited in).

It is important to point out that Lyapunov's stability theory is based on conventional solution theory, *i.e.*, the dynamic systems must be smooth. For the stability analysis of non-smooth systems, Lyapunov's second method needs to be extended. Paden and Sastry (1987) first generalized Lyapunov's second method by imposing a non-zero upper bound of the derivative of the Lyapunov function with respect to time. They proved that the states of the system (solution in the sense of Filippov) converge to the equilibrium point in a finite time.

Another extension of Lyapunov's stability theory based on Filippov's solution theory was done by Southwood et al. (1990) where the derivative of Lyapunov functions on the discontinuity surfaces were replaced with Dini-derivate. The most recent and systematic

extension of Lyapunov's second method for non-smooth dynamic systems was developed by Shevitz and Paden (1994) in which a non-smooth Lyapunov function is constructed. Their result is a theory applicable to systems with switches, for which Lyapunov functions are only piece-wise smooth.

The above extensions of Lyapunov's stability theory to non-smooth systems were based on the belief that non-smooth Lyapunov functions are natural for non-smooth dynamic systems. However, the main challenge in the construction of non-smooth Lyapunov functions is the evaluation of the derivatives of Lyapunov functions when the solution trajectories approach the discontinuity surfaces. Wu (1996) proved that if the existence and uniqueness of Filippov's solution are guaranteed, Lyapunov's second method can be applied directly to non-smooth dynamic systems. Furthermore, in reference (Wu *et al.* 1998b), a method is developed to construct smooth Lyapunov functions for non-smooth systems and it is shown that the construction of smooth Lyapunov functions is much easier for some engineering systems as compared to its non-smooth counterpart. The work was further extended for the determination of non-smooth Lyapunov functions (Wu and Sepehri 2001). Wu's work provided a solid framework in the study of posture stability and control of biped movement.

Lyapunov's stability theory has been used to analyze biped posture stability. Early work on the stability of biped models was restricted to small deviations about a vertical stance (Vukobratovic *et al.* 1970, Golliday and Hemami 1976, Hemami and Golliday 1977, Hemami and Cvetkovic 1977). Hemami and Wyman (1979) proposed a modeling and

control method to a constrained dynamic system with application to a three-link biped based on Lyapunov's linearization method. Feedback linearization and pole-assignment techniques were used for the control of such nonlinear systems. Iqbal *et al.* (1993) studied human postural and movement stability for simple voluntary movements, by means of a frontal four-link mathematic biped model. Hemami and Utkin (2002) studied Lyapunov stability of constrained and embedded rigid bodies. They presented a systematic method of stabilizing the systems and a procedure for constructing Lyapunov functions. Hemami *et al.* (2006) developed a quantitative framework to study the biomechanics and neural basis of the ankle strategy for maintaining posture stability. In their work, the stability of the biped was determined near the vertical stance by computing the poles, while the biped equations were linearized about the erect posture.

Although Lyapunov's second method is a powerful one, due to the lack of construction methods, it is difficult to derive a Lyapunov function for highly nonlinear systems. Thus, an alterative method is needed for the biped balance control (Wu *et al.* 2005). Sekhavat *et al.* (2004) employed the concept of Lyapunov exponents to analyze the stability of nonlinear dynamical systems and showed that the method is constructive and powerful. The concept of invariant exponents in the study of the stability of nonlinear differential equations was first introduced in 1889 by a Russian mathematician, Sonya Kovalevskaya, and was developed fully in 1892 by another Russian mathematician, Alexandr Mikhailovich Lyapunov.

The Lyapunov exponents have many important dimensions and computability directly

from data, without solving the differential or difference equations describing the corresponding dynamical systems (Kinsner 2003). A Lyapunov exponent is a number that reflects the rate of divergence or convergence, averaged over the entire attractor, of two neighboring state space trajectories. The calculation of the Lyapunov exponents can be grouped into two classes, mathematical models and time series.

Oseledec (1968) gave the theory of Lyapunov exponents in a form adapted to the needs of the theory of dynamical systems and of ergodic theory. Benettin *et al.* (1980) presented the theoretical results which are necessary for the numerical computation of all Lyapunov exponents. Wolf and collaborators (Wolf et al. 1985) described algorithms for calculating the spectrum of Lyapunov exponents from systems of which the equations are known. This model-based algorithm has been successfully applied to many smooth dynamic systems. Müller (1995) extended Wolf's method into non-smooth dynamic systems, *i.e.*, the ordinary differential equations contain non-differentiable terms. He pointed out that the required linearized equations have to be supplemented by certain transition conditions at the instances of discontinuities. Since Lyapunov exponents are calculated numerically over a long period of time, Mikens (2002), and Mikens and Gumel (2002) developed nonstandard finite difference techniques to improve numerical stability and computing efficiency (Sekhavat *et al.* 2005).

Yang and Wu (2006b) use Lyapunov exponents to analyze the stability of PD switching feedback control for biped standing, and determined a stability region. Ghorbani *et al.* (2007) employed Lyapunov exponents for stability analysis of a general regression neural

network (GRNN) feedback control which is used for balance-keeping during biped standing, and determined a stability region of this neural network controller. England and Granata (2007) quantified the local dynamic stability of a biped walking gait using maximum finite-time Lyapunov exponents $\lambda_{Max}$. A monotonic trend between $\lambda_{Max}$ and walking velocity was observed with smaller $\lambda_{Max}$ at slower walking velocities, which indicates more stable walking dynamics. The limitation of using mathematical models for the calculation of Lyapunov exponents is that the mathematical models are not always available. Even when mathematical models are available, the calculation of Lyapunov exponents can be unfeasible due to the models' complexity and uncertainties.

Another method for calculating Lyapunov exponents is based on time series. The most attractive advantage of using time series is that the data can often be measured experimentally without explicit knowledge of the dynamic models. The basic idea behind this method is to follow sets of trajectories over short time-spans and compute their rates of separation, then average those rates over the attractor. Wolf *et al.* (1985) described a computational method for approximating the largest Lyapunov exponents directly from the rate of separation of neighboring points. Sano and Sawada (1985) proposed a method to determine the spectrum of several Lyapunov exponents (including positive, zero, and even negative ones) from the observed time series of a single variable. Abarbanel *et al.* (1997) reviewed research on the calculation of Lyapunov exponents based on time series for chaotic systems. Sakai *et al.* (2003) analyzed the effect of extra reconstructed dimensions on the Lyapunov spectrum, which includes spurious Lyapunov exponents of unknown dynamical systems. This method is much better at calculating positive

exponents than negative ones, as the methods for calculating Lyapunov exponents based on a time series were developed primarily to analyze chaotic systems. The procedures are not reliable to calculate zero and negative exponents (Wolf *et al.* 1985) for potentially stable engineering systems.

In this work, the stability of the biped balance system is analyzed using the concept of Lyapunov exponents. The calculation of Lyapunov exponents is based on the mathematical model of the biped. In order to analyze the stability of complex or unknown systems using the concept of Lyapunov exponents, a new neural network approach is proposed. Neural networks are used to identify the system dynamics and then the Lyapunov exponents can be calculated based on the Jacobians, derived from the neural model.

### 1.2.4 System Identification Based on Neural Networks

System identification grew out of the statistics and engineering literature in the 1960s, motivated by the need to predict and control the behavior of complex systems (Box and Jenkins 1976). It is a method for using measured data to create or improve the mathematical model of the object being tested. It has been described as the process of selecting the mathematical model form and then, using measured test data, systemically adjusting the parameters based on predefined criterion, until the best possible correlation is achieved between the predicted and the measured response (Matzen and McNiven 1976). There have been a number of general references that range from the applied (Jenkins and Watts 1968, Ljung 1987) to the theoretical (Soderstrom and Stoica 1987) ends of the spectrum, as well as those which explicitly focus on the identification of

physiological systems (Marmarelis and Marmarelis 1978).

Central to the framework of system identification is the idea that components of a complex system can be represented as black boxes. As more is learned about a complex system, the goal becomes to reduce the relationship to smaller and smaller black boxes, until a sufficient level of detail has been achieved. This method is widely used in many research areas, such as civil engineering, electronic engineering, chemical engineering, etc. (Fukushima and Sugie 1999, Yue and Schlueter 2002, Kruglov *et al.* 2002, Bykov *et al.* 2003, Deng *et al.* 2003).

Neural networks provide an effective framework for the identification and control of nonlinear systems (Liu *et al.* 1989, Narendra and Parthasarathy 1990, Fang and Chow 2000). In recent years, considerable effort has been focused on the use of radial basis function neural networks (RBFNNs) (Chen and Billings 1992). Unlike multilayer perceptrons which originate from the field of biological science, RBFNNs are rooted primarily in the theory of multivariable functional interpolation in high-dimensional space (Broomhead and Lowe 1988, Powell 1985). It is a powerful computational tool, which has advantages of faster learning algorithms, better approximation capabilities and local minimum problem avoidance (Ai-Amoudia and Zhang 2000, Gomm and Yu 2000, Rank 2003). It can identify relatively high-order systems and has increasingly been used in many practical areas such as control, signal processing, pattern recognition, systems identification and time series prediction.

RBFNNs tend to have improved training characteristics in comparison to standard feed-forward neural networks, due to their localized nature and the fact that they are linear in weight (Gorinevski 1996). They can also be made compact by having the number of points about which the radial basis functions are centered, grow and shrink, to obtain a minimal network (Platt 1991, Kadirkanmanathan and Niranjan 1993, Yingwei *et al.* 1997). Various functions have been investigated and used as the radial basis function (RBF) for RBFNN, including Gaussian function (Schagen 1986), thin-plate splines (Duchon 1977), multi-quadratics (Hardy 1971) and inverse multi-quadratic functions (Powell 1987).

The original RBFNN requires that there be as many as hidden units, known as the RBF centers as the data points, which is prohibitively expensive to implement in computational terms when the number of data points is high. Several methods have been proposed to overcome this difficulty. Poggio and Girosi (1990) provided an approximate approach which involves searching for a suboptimal solution in a lower-dimensional space. This is done by using a standard technique known in variational problems as the Galerkin method. Moody and Darken (1989) developed a method in which the RBF centers are chosen in a self-organized fashion. Chen *et al.* (1991) suggested using an orthogonal Least Squares Learning algorithm to choose the RBF centers from data points. The selected centre maximizes the increment to the explained variance of the desired outputs and the algorithm does not suffer numerical ill-conditioning problems. All of these effects have focused on the selection and computation of the RBF centers.

Another important component of the RBF network is weight. Langari and Wang (1995)

proposed a modified RBF network in which the regression weights are used to replace the constant weights in the output layer that can reduce the number of hidden units significantly.

## 1.3 Objectives

There are two objectives in this research. The first is, to design two balance systems that enable a biped robot to remain in an upright posture during standing. The standing biped is modeled as a two-link inverted pendulums presenting the leg and the torso with a foot-link. Two optimal controllers are developed. An LQR balance controller is designed to minimize the torque outputs of the control system. A GA-based PD controller is used to ensure the satisfaction of the constraints between the foot-link and the ground as well as optimize the energy consumption of the control systems. The second objective, is to analyze the stability of the proposed control systems using the concept of Lyapunov exponents.

In this work, the stability region of the biped balance systems is also determined using the concept of Lyapunov exponents. A new method is proposed to determine Jacobians for complex or unknown systems, a basic requirement in the calculation of Lyapunov exponents. RBFNNs have been employed to identify the biped balance systems. Then, the numerical Jacobians can be derived from the neural model for the calculation of Lyapunov exponents.

## 1.4 Thesis Organization

The remainder of this thesis is divided into four chapters. A description of each is outlined below:

**Chapter 2** introduces the background and key concepts of Lyapunov exponents and system identification using neural networks. This chapter also describes the methodology used to calculate Lyapunov exponents for the biped balance system based on neural network identification. The biped model and the feet constraints during biped standing are discussed as well.

**Chapter 3** describes a classical feedback state balance control system using a linear quadratic regulator (LQR) technique. The stability of the proposed controller is analyzed using the concept of Lyapunov exponents and the stability region is determined. In simulation, the results of Lyapunov exponents based on the neural model are compared to the results based on the mathematical model.

**Chapter 4** details a GA-based PD balance control system for biped standing. GA is employed to ensure the satisfaction of the feet constraints as well as to optimize the total energy consumption of the torque outputs. The stability of the proposed controller is analyzed using the concept of Lyapunov exponents and the stability region is determined. The results of Lyapunov exponents based on the neural model, and the mathematical model are compared.

**Chapter 5** discusses and evaluates the proposed balance systems and the Lyapunov

exponents as a tool for stability analysis. It will also draw conclusions about system identification based on neural networks, and recommended future developments are outlined.

# Chapter 2

# The Calculation of Lyapunov Exponents Based on Neural Models

## 2.1 Introduction

The concept of Lyapunov exponents is an important tool in categorizing the steady-state behavior of dynamical systems, determining instability of the systems, classifying invariant sets and approximating the dimension of strange attractors or other nontrivial invariant sets. It works for discrete as well as continuous systems.

The calculation of Lyapunov exponents can be carried out using two approaches. One is based on the mathematic models of physical systems. However, such models are not always available. Even if they are obtained, deriving system Jacobians, which is crucial in the calculation of Lyapunov exponents, can be unfeasible due to the model complexities. The other method for calculating Lyapunov exponents is based on a time series which can be measured experimentally. This method is currently used for analyzing unknown systems without explicit knowledge of the mathematic models. This method has been

developed primarily to analyze chaotic system. It is not reliable for calculating zero and negative exponents (Wolf 1985). This is because the linear analysis used in the method becomes totally inaccurate when the displacement due to local data-set curvature is comparable to the thickness of the data set. In order to solve the above problems, a new approach, where neural networks are used to identify the physical system, is developed.

In this work, radial basis function neural networks (RBFNNs) are employed due to their capacity for nonlinear system identification. This neural model will be used to derive the Jacobians and used as the mathematical model of the system. This allows the Lyapunov exponents to be determined using the first method, which is based on mathematical models. This proposed approach can avoid the complexity of deriving Jacobians. For the calculation of Lyapunov exponents based on a time series, the proposed approach can be an alternate method.

This chapter is organized as follows. Section 2.2 introduces the concept of Lyapunov exponents and the method to calculate Lyapunov exponents based on mathematical models. Section 2.3 describes the structure of RBFNN and the approach to derive Jacobians from neural models. Biped balance systems are used to demonstrate the efficiency of the proposed neural method in Section 2.4.

## 2.2 Stability Analysis Using the Concept of Lyapunov Exponents

### 2.2.1 The Concept of Lyapunov Exponents

Lyapunov exponents (or characteristic numbers) were first introduced by Lyapunov (Lyapunov 1892) in order to study the stability of non-stationary solutions of ordinary differential equations (ODEs). They have since been extensively studied in the literature to diagnose chaotic systems (Dieci *et al.* 1997). As described in the work of Oseledec (1968), the concept of Lyapunov exponents provides a meaningful way to characterize the asymptotic behavior of a nonlinear dynamical system. Wolf *et al.* (1985) defined the spectrum of Lyapunov exponents in the manner most relevant to spectral calculations.

Given a smooth dynamical system in an n-dimensional state space as shown below:

$$\dot{x} = f(x,t), \quad x(0) = x_0, x \in R^n \tag{2.1}$$

where $x = \{x_1,...,x_n\}^T$ is the state vector, and $f(x,t)$ is a continuously differentiable vector function. When monitoring the long-term evolution of an infinitesimal $n$-sphere of initial conditions, the sphere will become an $n$-ellipsoid due to the locally deforming nature of the flow. The $i^{th}$ dimensional Lyapunov exponent is then defined in terms of the length of the ellipsoidal principal axis $\|\delta x_i(t)\|$ as follows:

$$\lambda_i = \lim_{t\to\infty}\left[\frac{1}{t}\ln\frac{\|\delta x_i(t)\|}{\|\delta x_i(t_0)\|}\right] \qquad (i=1,\ldots,n) \tag{2.2}$$

where $\lambda_i$ is ordered from largest to smallest. $\|\delta x_i(t_0)\|$ and $\|\delta x_i(t)\|$ denote the lengths of

the $i^{th}$ principal axis of the infinitesimal $n$-dimensional hyper-ellipsoid at initial and current time instances, $t_0$ and $t$, respectively.

The concept of Lyapunov exponents provides a generalization of the linear stability analysis for perturbations of steady state solutions to time-dependent solutions. Lyapunov exponents are global properties and independent of the trajectory chosen to calculate them (the fiducial trajectory). This independence is a consequence of a theorem of Oseledec (Oseledec 1968), which applies in the limit of infinite time. However, in practical application, we are usually dealing with finite-time Lyapunov exponents, which are defined as:

$$\lambda_i = \frac{1}{t} \ln \frac{\|\delta x_i(t)\|}{\|\delta x_i(t_0)\|} \quad (i=1,\ldots,n) \tag{2.3}$$

In the limit as time $t \to \infty$, the finite-time Lyapunov exponents converge to the true Lyapunov exponents (Thiffeault and Boozer 2001).

The above definition of Lyapunov exponents indicates that Lyapunov exponents, $\lambda_i$ ($i$=1,...,$n$), are the average exponential rates of divergence or convergence of nearby orbits in the state space where $n$ is the number of Lyapunov exponents, which is equal to the dimension of the state space of the system. The Lyapunov exponents are related to the expanding or contracting nature of different directions in the state space. Since the orientation of the ellipsoid changes continuously as it evolves, the directions associated with a given exponent vary in a complicated way through the attractor. Therefore, one cannot speak of a well-defined direction associated with a given exponent.

A common approach in visualizing state-space motion is to imagine how a small length, area, or higher-dimensional element might evolve in time. An example of such elements is an initially infinitesimal ball that has a radius $\delta x(0)$ at time $t = 0$ (in three-dimensional state space). As the ball evolves under the action of a non-uniform flow it will eventually distort. Since we have assumed an infinitesimal state-space element, the change in space, we presume, will be determined only by the linear part of the flow. It remains an ellipsoid as it evolves.

$\delta x_i(t)$ is the $i^{th}$ ($i$=1,2 and 3) member of the set of the principal axes of the ellipsoid at time. The end-points of each principal axis are considered to be neighboring points in the state-space. We measure the growth or shrinkage of each principal axis $\delta x_i(t)$ over the entire attractor, according to whether its endpoints get closer or farther apart. That means that we get a Lyapunov exponent for each principal axis. The largest Lyapunov exponent measures the rate of expansion of the first principal axis - the one that shows the largest amount of growth (or the slowest rate of shrinkage) over the attractor. The second Lyapunov exponent measures the rate of change of the second principal axis, and so on down to the smallest Lyapunov exponent (Williams 1997).

The concept of Lyapunov exponents is an important tool in categorizing steady-state behavior in a dynamic system, determining instability of the system, classifying invariant sets and approximating the dimension of strange attractors or other nontrivial invariant sets (Wolf *et al.* 1985, Müller 1995, Williams 1997). A negative Lyapunov exponent

indicates an average convergence of trajectories; a positive exponent indicates an average divergence. Negative Lyapunov exponents typify non-chaotic attractors. At least one positive Lyapunov exponent usually happens only on chaotic attractors.

In dissipative systems, an attractor with one or more positive Lyapunov exponents is generally said to be strange or chaotic. Based on the fact that (i) one Lyapunov exponent of any limit set other than an equilibrium point must be zero, and (ii) the sum of the Lyapunov exponents of dissipative systems must be negative, the hyperbolic attractors can be classified as follows (Williams 1997):

- For an exponentially stable equilibrium point, $\lambda_i<0$ ($i$=1,...,n)
- For an exponentially stable limit cycle, $\lambda_1=0$ and $\lambda_i<0$ ($i$=2,...,n)
- For an exponentially stable k-torus, $\lambda_i=...=\lambda_k=0$ and $\lambda_i<0$ ($i=k+1$,...,n)
- For a chaotic attractor, $\lambda_1>0$ and $\sum\lambda_i<0$ ($i$ = 1,...,n)

Using a 2D state space as an example, the Lyapunov exponents of dynamic systems can be classified as follows:

(a) $\lambda_i < 0$: The orbit attracts to a stable fixed point. Negative Lyapunov exponents are characteristic of dissipative or non-conservative systems (the damped harmonic oscillator for instance). Such systems exhibit exponential stability; the more negative the exponent, the faster the systems move to the steady state. Super-stable fixed points have a Lyapunov exponent of $\lambda_i = -\infty$. This is akin to a critically damped oscillator in that the system heads towards its equilibrium point as quickly as possible. Nearby points on the trajectory will converge closer and closer as shown in Figure 2.1(a).

(b) $\lambda_i = 0$: A Lyapunov exponent of zero indicates that the system is in some sort of steady state mode. A physical system with this exponent is conservative. Such systems exhibit stability in the Lyapunov sense. Nearby points on the trajectory will stay at the separation all of the time, as shown in Figure 2.1(b).

(c) $\lambda_i > 0$: The orbit is unstable. No matter how close, nearby points on the trajectory will diverge to arbitrary separation, as shown in Figure 2.1(c).

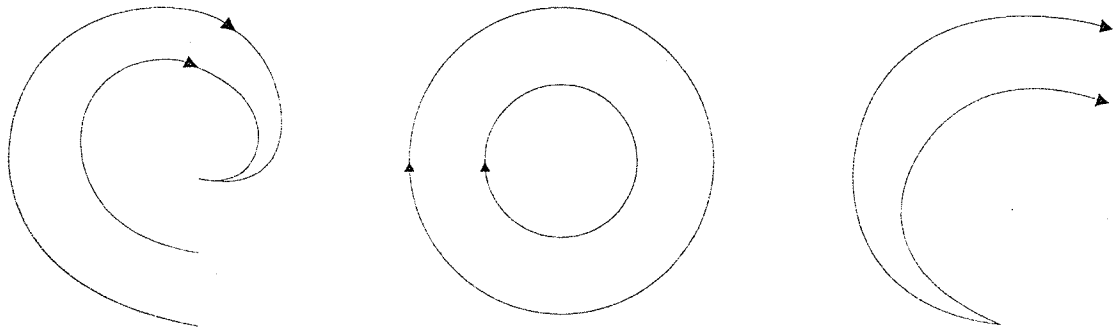

(a) $\lambda_i$<0 (b) $\lambda_i$=0 (a) $\lambda_i$>0

Figure 2.1 Different orbits projected on the $i^{th}$ dimension different Lyapunov exponents

### 2.2.2 The Calculation of Lyapunov Exponents Based on Mathematical Models

Lyapunov exponents are defined by the long-term evolution of the axes of an infinitesimal sphere of states. Wolf *et al.*, (1985) developed algorithms for calculating the spectrum of Lyapunov exponents from systems where the dynamic equations are known. The procedure of calculating Lyapunov exponents from differential equations can be implemented by defining the principal axes with initial conditions whose separations are

as small as the computer limitation allows, and evolving such principal axes with the nonlinear equations of motion. A "fiducial" trajectory (the center of the sphere) is defined by the action of the nonlinear equations of motion on some initial conditions. The trajectories of points on the surface of the sphere are defined by the action of the linearized equations of motion on points infinitesimally separated from the fiducial trajectory. In particular, the principal axes are defined by the evolution via the linearized equations of an initially orthonormal vector frame anchored to the fiducial trajectory. This leads to the following set of equations (Wolf *et al.* 1985).

$$\begin{Bmatrix} \dot{x}(t) \\ \dot{\psi}_{x(t)} \end{Bmatrix} = \begin{Bmatrix} f(x(t)) \\ J(x(t))\psi_{x(t)} \end{Bmatrix} \tag{2.4}$$

where $\psi_{x(t)}$ is called the state transition matrix of the linearized system $\delta x(t) = \psi_{x(t)}\delta x(0)$ and the variation equation, $\dot{\psi}_{x(t)} = J(x(t))\psi_{x(t)}$, is a matrix-valued time-varying linear differential equation. It is derived by the linearization of the vector field along the trajectory $x(t)$. The Jacobian $J(x(t))$ is defined as

$$J(x(t)) = \left.\frac{\partial \dot{x}}{\partial x}\right|_{x=x(t)} = \left.\frac{\partial f(x)}{\partial x}\right|_{x=x(t)} \tag{2.5}$$

The initial conditions for numerical integrations are $\begin{Bmatrix} x(t_0) \\ \psi_{x(t)}(t_0) \end{Bmatrix} = \begin{Bmatrix} x_0 \\ I \end{Bmatrix}$ where $I$ is the identify matrix.

Lyapunov exponents are calculated by following the evolution of the volume of the hyper-ellipsoid spanned by $\delta x_i$ ($i$=1,...,$n$), via separately following the evolution of $\delta x_i$ using an integration method. However the vectors $\delta x_1, \delta x_2, ..., \delta x_n$ may tend to align as

$t \to \infty$. This alignment makes the calculations unreliable (Parker and Chua 1989). To solve the problem, $\delta x_1(t), \delta x_2(t), ..., \delta x_n(t)$ are reorthonormalized at each integration step. This is done by including the Gram-Schmidt Reorthonormalization (GSR) scheme in the calculation procedure. Gram-Schmidt reorthonormalization generates an orthonormal set $\{u_1, ..., u_n\}$ of $n$ vectors with the property that $\{u_1, ..., u_n\}$ spans the same subspace as $\{\delta x_1, ..., \delta x_n\}$.

Figure 2.2 shows the geometrical interpretation of the orthonormalization for $\delta x_1(k)$ and $\delta x_2(k)$ ($k$=1,...,$K$ and $K$ is the number of integration steps). They are orthogonalized into $v_1(k)$ and $v_2(k)$, then normalized into $u_1(k)$ and $u_2(k)$.

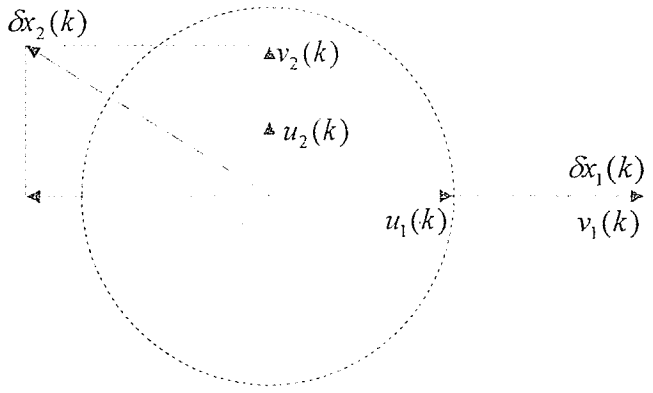


Figure 2.2 Orthonormalization of two vectors $\delta x_1(k)$ and $\delta x_2(k)$

Let the linearized equations of motion, act on the initial frame of orthonormal vectors to give a set of vectors $\{\delta x_1, \delta x_2, ..., \delta x_n\}$. The orientation-preserving properties of GSR mean that the initial labeling of the vectors may be done arbitrarily. The GSR provides the following orthonormal set $\{u_1, u_2, ..., u_n\}$ as defined below:

$$v_1 = \delta x_1, \quad u_1 = \frac{v_1}{\|v_1\|}$$

$$v_2 = \delta x_2 - \langle \delta x_2, u_1 \rangle u_1, \quad u_2 = \frac{v_2}{\|v_2\|}$$

...

$$v_n = \delta x_n - \langle \delta x_n, u_1 \rangle u_1 - \ldots - \langle \delta x_n, u_{n-1} \rangle u_{n-1}, \quad u_n = \frac{v_n}{\|v_n\|} \tag{2.6}$$

Where $\langle , \rangle$ signifies the inner product. GSR procedure allows the integration of the vector frame for as long as required for Lyapunov spectrum convergence. At the $K^{th}$ state, the GSR procedure produces orthonormal vector frame $\{u_1, u_2, \ldots, u_n\}$, and for the $K$ chosen large enough, the Lyapunov exponents are:

$$\begin{cases} \lambda_1 \approx \dfrac{1}{Kh} \sum_{k=1}^{K} \ln \|u_1(k)\| \\ \lambda_2 \approx \dfrac{1}{Kh} \sum_{k=1}^{K} \ln \|u_2(k)\| \\ \cdots \\ \lambda_n \approx \dfrac{1}{Kh} \sum_{k=1}^{K} \ln \|u_n(k)\| \end{cases} \tag{2.7}$$

where $h$ is the time-step size.

This model-based algorithm described by Wolf and his collaborators (Wolf *et al.* 1985) has been successfully applied to many dynamic systems. Sekhavat (Sekhavat 2004) demonstrated the above procedure of calculating Lyapunov exponents on the simple three-dimensional Lorenz system. Yang and Wu (Yang and Wu 2006a) used the concept of Lyapunov exponents to analyze the stability of a PD-based switching state balance control during biped standing.

Overall, the procedure for calculating of Lyapunov exponents based on a mathematic model is described as follows:

Step1: Choosing initial conditions for the nonlinear system and the linear system (orthonormal frame) as shown in Equation (2.4)

Step2: Integrating nonlinear and linear equations simultaneously, obtaining the initial states for the next step.

Step 3: Using GSR procedure to obtain the reorthonormal frame using Equation (2.6).

Step 4: Calculating Lyapunov exponents by Equation (2.7).

Step 5: Repeating Step 2 to Step 4, until convergent values of Lyapunov exponents are obtained.

The most difficult part in the calculation of Lyapunov exponents; is deriving Jacobians in Equation (2.5) for complex or unknown systems. In order to solve this problem, the next section presents a neural approach to derive Jacobians based on RBFNN system identification.

## 2.3 System Identification Based on Neural Networks

In order to analyze the stability of complex or unknown systems using the concept of Lyapunov exponents, system identification is required for the determination of the Jacobian matrices. System identification is the process of building good models of dynamic systems based on measured data from the actual processes. The mathematical

model in this case is the black box, which describes the relationship between the input and output signals. To adequately model the systems, neural networks must be used. Previous studies in system identification have demonstrated that neural networks are successful in modeling many non-linear systems, by comparing simulated data with real data (Chen *et al.* 1992).

### 2.3.1 Radial Basis Function Neural Network (RBFNN)

Unlike multilayer perceptions which originate from the field of biological science, radial basis function neural networks (RBFNNs) are rooted primarily in the theory of multi-variable functional interpolation in the high-dimensional space. The architecture of the radial basis function network is a multilayer feed-forward network that consists of three layers, the input, the hidden and the output layers. A typical RBFNN configuration with a single output is shown in Figure 2.3.

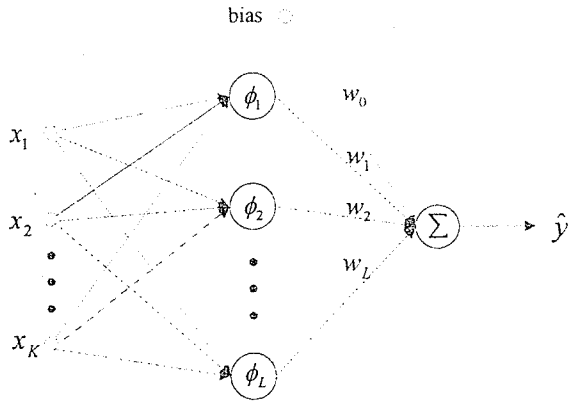


Figure 2.3 Typical RBFNN architecture

The input layer connects the network to the environment. $X=\{x_1,x_2,...,x_K\}$ is the input feature vector, where $K$ is the number of input units. The second layer applied a nonlinear

transformation (activation function) from the input space to the hidden space, which is highly dimensional. Various functions have been tested to serve as the activation functions for RBFNN (Chen 1991). In system identification applications, the Gaussian function is preferred (Bors and Gabbouj 1994). It is supposed that, the radial vector of RBFNN adopts multivariable Gaussian function. The centers are usually chosen to be a subset of the data or distributed uniformly in the input domain. The output of hidden neuron $j$ is denoted by $\phi_j$ and is given by

$$\phi_j = \exp(-\frac{\|X - C_j\|^2}{2b_j^2}), \quad j=1,2,...,L \tag{2.8}$$

where $L$ are the numbers of hidden units. $C_j=\{c_1,c_2,...,c_K\}$ is the center vector for neuron $j$. In the basic form, all inputs are connected to each hidden neuron and the norm is typically taken to be the Euclidean distance. Geometrically, a radial basis function represents a bump in the multidimensional space as shown in Figure 2.4, whose dimension is given by the number of entries.

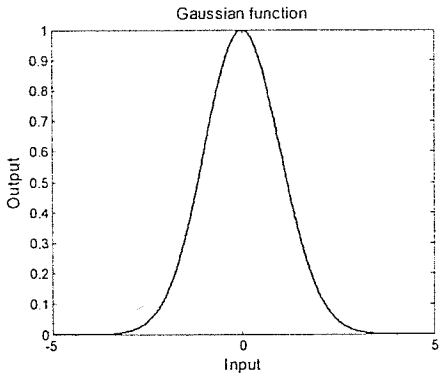


Figure 2.4 Gaussian function

The output units $\hat{y}$ implement a weighted sum of hidden unit outputs:

$$\hat{y} = w_0 \times bias + \sum_{j=1}^{L} w_j \phi_j \tag{2.9}$$

where $w_j$ are the output weights, each corresponding to the connection between a hidden unit and an output unit. The weights $w_j$ show the contribution of a hidden unit to the respective output unit. This is impractical and it would be easier if only one of the parameters were adjusted. To cope with this problem a bias neuron is used. The bias neuron lies in one layer. It is connected to all of the neurons in the next layer, but none in the previous layer and it always emits 1. Since the bias neuron emits 1, the weights connected to the bias neuron are added directly to the combined sum of the other weights.

RBFNNs are characterized by their localization (center) and by an activation hypersurface. In the case of Gaussian functions these are centered about a grid point $C_j$ and scaled by a coefficient parameter $b_j$. The activation function $\phi_j$ influence, decreases according to the Euclidean distance from the center $C_j$. For high-precision grids, these weights $w_j$ effectively mould the input–output behavior of the RBFNN to that of the system being identified. For low-precision grids, the computed weights $w_j$ serve as an effective initial guess for a learning algorithm based on the least mean plant output at time $n$ which can be pre-computed. This means that data samples located at a large Euclidean distance from the RBF center will fail to activate that basic function. The maximum activation is achieved when the data sample coincides with the center vector.

### 2.3.2 RBFNNs Training Algorithms

By means of training, the neural network models the underlying function of a certain mapping. In order to model such a mapping, we have to find the network weights and topology. There are two categories of training algorithms: supervised and unsupervised.

In a supervised application, we are provided with a set of data samples called a "training set" for which the corresponding network outputs are known. In this case the network parameters are found such that, they minimize a cost function:

$$E = \frac{1}{2}(y - \hat{y})^2 \tag{2.10}$$

where $\hat{y}$ denotes the RBF output vector and $y$ represents the output vector associated with the a data sample $X$ from the training set. An adaptive training algorithm for minimizing a given cost function is a gradient descent algorithm with momentum. The gradient descent method is an iterative method for finding a local minimum of some function.

Assume that we have a function $f(x)$ and that we start out in $x(0)$ having the value $f(x(0))$. We wish to find a configuration $x(m)$, where $f(x)$ attains its minimum value. To do this, we can iteratively update the point we stand in by going in the opposite direction of the gradient of $f(x)$. The direction of the gradient is the direction which increases $f(x)$ the most. Recalling that the gradient of a function is the partial derivatives with respect to the variables in the function as

$$\nabla f(x) = \frac{\partial f(x)}{\partial x} \tag{2.11}$$

During the iteration, if the step size with which we update our current position is too big we might fail to reach the minimum. Therefore, in order to control the movement rate at each iteration; we introduce a learning rate $\mu$. The general procedure can now be written at epoch $k+1$ as follows:

$$x(k+1) = x(k) - \mu \nabla f\big(x(k)\big) \tag{2.12}$$

where $\nabla f(x(k)) = \frac{\partial f(x(k))}{\partial x(k)}$. The algorithm stops when the position $x$ has not changed after an iteration, in which case we have arrived at a local minimum. This process is illustrated in the following Figure 2.5. Note that, we cannot say whether or not the minimum we have arrived in, is actually the global minimum.

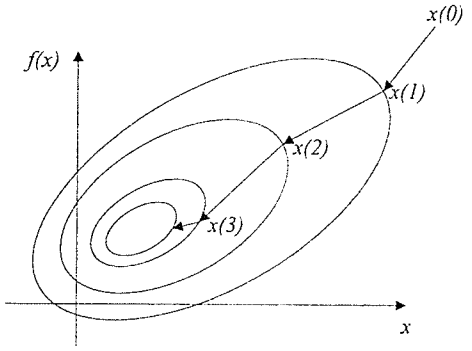


Figure 2.5 Gradient descent algorithm

To make this method an order of magnitude more efficient; we can modify the learning algorithm to include an extra term

$$x(k+1) = x(k) - \mu \nabla f(x(k)) + \eta \Delta f(x(k)) \tag{2.13}$$

where $\Delta f(x(k)) = f(x(k)) - f(x(k-1))$, $\eta$ is the momentum constant. $\eta \Delta f(x(k))$ is generally called the momentum term and has two functions. First, it can smooth out local irregularities in the minimization function allowing the gradient descent to follow a consistent path. Secondly, it allows the minimization process to increase in speed when there are long periods of identical gradient evaluations. Gradient descent with momentum allows a network to respond not only to the local gradient, but also to recent trends in the error surface. Acting like a low-pass filter, momentum allows the network to ignore small features in the error surface. Without momentum, a network can get stuck in a shallow

local minimum. With momentum, a network can slide through such a minimum.

Gradient descent with momentum depends on two training parameters $\mu$ and $\eta$. $\eta$ is set between 0 (no momentum) and values close to 1 (lots of momentum). A momentum constant of 1, results in a network that is completely insensitive to the local gradient and therefore, does not learn properly. The centers of the RBFNN are initialized randomly.

By connecting the neurons in a layered array, we can derive the RBF algorithm based on the gradient descent with momentum method described as follows:

Step 1: Find the error $E(k)=\frac{1}{2}(y(k)-\hat{y}(k))^2$ at step $k$.

Step 2: Change the connection weights in the output layer and hidden layer in the following way:

$$w_j(k+1)=w_j(k)-\mu\nabla w_j(k)+\eta\Delta w_j(k)$$
$$b_j(k+1)=b_j(k)-\mu\nabla b_j(k)+\eta\Delta b_j(k)$$
$$c_{ji}(k+1)=c_{ji}(k)-\mu\nabla c_{ji}(k)+\eta\Delta c_{ji}(k)$$

where:

$$\nabla w_j(k)=\frac{\partial E(k)}{\partial w_j(k)}=\frac{\partial E(k)}{\partial \hat{y}(k)}\frac{\partial \hat{y}(k)}{\partial w_j(k)}=-\big(y(k)-\hat{y}(k)\big)\phi_j(k)$$

$$\Delta w_j(k)=w_j(k)-w_j(k-1)$$

$$\nabla b_j(k)=\frac{\partial E(k)}{\partial b_j(k)}=\frac{\partial E(k)}{\partial \hat{y}(k)}\frac{\partial \hat{y}(k)}{\partial \phi_j(k)}\frac{\partial \phi_j(k)}{\partial b_j(k)}=-(y(k)-\hat{y}(k))w_j(k)\phi_j(k)\frac{\|X(k)-C_j(k)\|^2}{b_j(k)^3}$$

$$\Delta b_j(k)=b_j(k)-b_j(k-1)$$

$$\nabla c_{ji}(k)=\frac{\partial E(k)}{\partial c_{ji}(k)}=\frac{\partial E(k)}{\partial \hat{y}(k)}\frac{\partial \hat{y}(k)}{\partial \phi_j(k)}\frac{\partial \phi_j(k)}{\partial c_{ji}(k)}=-(y(k)-\hat{y}(k))w_j(k)\phi_j(k)\frac{x_i(k)-c_{ji}(k)}{b_j{}^2(k)}$$

$$\Delta c_{ji}(k) = c_{ji}(k) - c_{ji}(k-1) \tag{2.14}$$

Step 3: If the error becomes lower than a predetermined value, stop the training. Otherwise, replace $k$ by $k+1$ and go to step 1.

In unsupervised training, the output assignment is not available for the given set. A large variety of training algorithms has been tested for training RBFNN. In the initial approaches, each data sample was assigned to a basis function. This solution proved to be expensive in terms of memory requirement and in the number of parameters. On the other hand, an exact fit to the training data may cause bad generalizations. Other approaches choose randomly or assumed known hidden unit weights, and calculate the output weights $w_j$ by solving a system of equations whose solution is given in the training set (Broomhead and Lowe 1988). The matrix inversion required in this approach is computationally expensive and could cause numerical problems in certain situations (when the matrix is singular). In some previous work (Matej and Lewitt 1996, Sanner and Slotine 1994), the radial basis function centers are uniformly distributed in the data space. The function to be modeled is obtained by interpolation.

### 2.3.3 The Determination of System Jacobians Based on RBFNN Models

In this chapter, RBFNN is employed to identify unknown systems, where the output continuously depends on the past input and past output. The inputs of RBFNN are the same as the state variables of the plant $x(n)$ at step $n$. The outputs are the state rate of the plant $\dot{x}(n+1)$ at next step $n+1$:

$$\dot{x}(n) = \frac{x(n) - x(n-1)}{h} \tag{2.15}$$

where $h$ is the sampling rate. After extensive training, the RBFNN model of the system under study can be developed. Such a model is to be used to determine the Jacobian $J$. For example, the Jacobian of the output $k$, corresponding to the input $i$, is given as follows:

$$J_{ki}(n) = \frac{\partial \dot{x}_k(n)}{\partial x_i(n-1)} \approx \frac{\partial \hat{\dot{x}}_k(n)}{\partial x_i(n-1)} = \sum_{j=1}^{L} w_{kj}\phi_{kj}\frac{c_{kji} - x_{ki}(n-1)}{b_{kj}^2} \tag{2.16}$$

The Lyapunov exponents can be calculated based on the above neural Jacobians. The accuracy of the Lyapunov exponents depends on the neural model. The training of RBFNN is a key issue for this method. In the next section, a biped balance system is shown as an example to train RBFNN.

## 2.4 Case Study: Biped Balance System

In this work, a biped robot is simplified as a two-link inverted pendulum system with one rigid foot-link, as shown in Figure 2.6. Link 1 represents the leg and link 2 represents the torso. The joints 1 and 2 are equivalent to the ankle and hip joints. The foot-link provides a support based on the ground. The biped is assumed to move in the sagittal plane. This model is simple but adequate for studying the dynamics and control of the biped during standing.

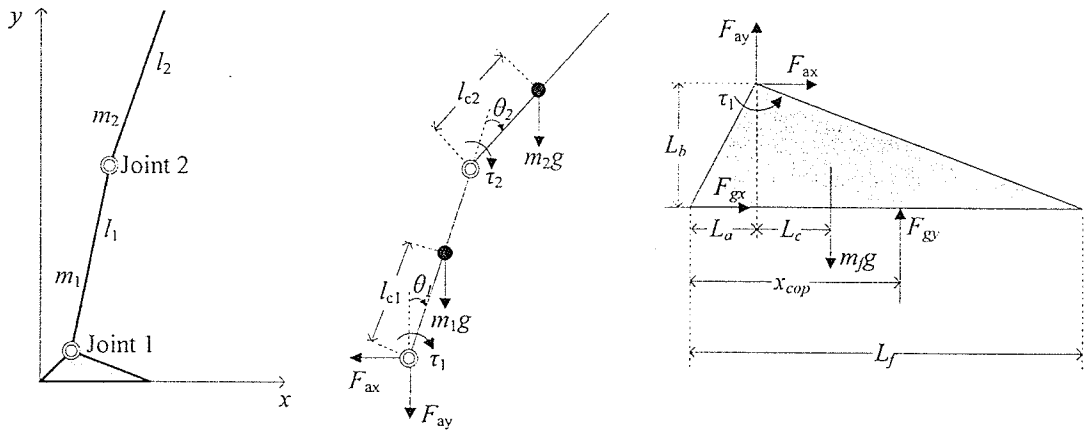


Figure 2.6. (a) simplified biped model, (b) free body diagram of the two link inverted pendulum, and (c) free body diagram of the foot-link

The model parameters $m_i$, $l_i$, $l_{ci}$ $I_i$ ($i$=1,2) are the mass, length, location of mass center and moment of inertia of the link $i$. $L_f$, $L_a$, $L_b$, $L_c$ are the length of the foot, horizontal distance between the ankle and the heel, ankle height, horizontal distance between the mass center of the foot and the ankle. $x_{cop}$ is the location of the center of pressure (COP) to the heel. $\theta_1$ and $\theta_2$ are the two joint angles which are positive in the clockwise direction. $\tau_1$ and $\tau_2$ are the control torques applied at both joints, which are positive in the clockwise direction. $g$ is the gravitational acceleration. Supposing that there is no friction, the equation of motion can be derived from the Lagrangian formulation as follows:

$$\tau = D(\theta)\ddot{\theta} + C(\theta,\dot{\theta})\dot{\theta} + G(\theta) \tag{2.17}$$

where $\tau = [\tau_1, \tau_2]^T$ , $\theta = [\theta_1, \theta_2]^T$ , $\dot{\theta} = [\dot{\theta}_1, \dot{\theta}_2]^T$ and $\ddot{\theta} = [\ddot{\theta}_1, \ddot{\theta}_2]^T$ .The terms $D(\theta)$ , $C(\theta,\dot{\theta})$ and $G(\theta)$ can be represented as follows:

$$D(\theta) = \begin{bmatrix} d_{11} & d_{12} \\ d_{21} & d_{22} \end{bmatrix}$$

$$d_{11} = m_1 l_{c1}^2 + m_2 l_1^2 + m_2 l_{c2}^2 + 2m_2 l_1 l_{c2} \cos\theta_2 + I_1 + I_2$$

$$d_{12} = d_{21} = m_2 l_{c2}^2 + m_2 l_1 l_{c2} \cos\theta_2 + I_2$$

$$d_{22} = m_2 l_{c2}^2 + I_2$$

$$C(\theta,\dot{\theta}) = \begin{bmatrix} -m_2 l_1 l_{c2}\dot{\theta}_2 \sin\theta_2 & -m_2 l_1 l_{c2}(\dot{\theta}_1 + \dot{\theta}_2)\sin\theta_2 \\ m_2 l_1 l_{c2}\dot{\theta}_1 \sin\theta_2 & 0 \end{bmatrix}$$

$$G(\theta) = \begin{bmatrix} -(m_1 l_{c1} + m_2 l_1) g \sin\theta_1 - m_2 l_{c2} g \sin(\theta_1 + \theta_2) \\ -m_2 l_{c2} g \sin(\theta_1 + \theta_2) \end{bmatrix} \tag{2.18}$$

If we defined $q = [q_1, q_2, q_3, q_4] = [\theta_1, \theta_2, \dot{\theta}_1, \dot{\theta}_2]$, the state-space model of the biped balance system becomes

$$\dot{q}_1 = q_3$$

$$\dot{q}_2 = q_4$$

$$\begin{aligned} \dot{q}_3 = \Bigg[ & \delta\tau_1 - (\delta + \frac{\beta}{2}\cos q_2)\tau_2 + \left(\delta(q_3 + q_4)^2 + \frac{\beta}{2} q_3^2 \cos q_2\right)\frac{\beta}{2}\sin q_2 \\ & - \left(\frac{\beta}{2} m_2 l_{c2} \cos q_2 \sin(q_1 + q_2) - \delta(m_1 l_{c1} + m_2 l_1)\sin q_1\right) g \Bigg] / D \end{aligned} \tag{2.19}$$

$$\begin{aligned} \dot{q}_4 = \Bigg[ & -(\alpha + \frac{\beta}{2}\cos q_2)\tau_1 + (\alpha + \beta\cos q_2)\tau_2 \\ & - \frac{\beta}{2}\sin q_2 \left((\delta + \frac{\beta}{2}\cos q_2)(q_3 + q_4)^2 + (\alpha - \delta + \frac{\beta}{2}\cos q_2) q_3^2\right) \\ & + \left(-(\delta + \frac{\beta}{2}\cos q_2)(m_1 l_{c1} + m_2 l_1)\sin q_1 + (\alpha - \delta + \frac{\beta}{2}\cos q_2) m_2 l_{c2} \sin(q_1 + q_2)\right) g \Bigg] / D \end{aligned}$$

where

$$D = m_1 m_2 l_{c1}^2 l_{c2}^2 + m_1 l_{c1}^2 I_2 + m_2 l_{c2}^2 I_1 + m_2^2 l_{c2}^2 l_1^2 + m_2 l_1^2 I_1 + I_1 I_2 - m_2^2 l_{c2}^2 l_1^2 \cos^2 q_2$$

$$\alpha = m_1 a_1^2 + m_2 l_1^2 + m_2 l_{c2}^2 + I_1 + I_2$$

$$\beta = 2 m_2 l_1 l_{c2}$$

$$\delta = m_2 l_{c2}^2 + I_2$$

Using Newton's second and third laws, the horizontal and vertical ground reaction forces are given as:

$$F_{gx} = m_1\ddot{x}_1 + m_2\ddot{x}_2 \tag{2.20}$$

$$F_{gy} = m_1\ddot{y}_1 + m_2\ddot{y}_2 + (m_1 + m_2 + m_f)g \tag{2.21}$$

where

$$\ddot{x}_1 = -l_{c1}\sin\theta_1\dot{\theta}_1^2 + l_{c1}\cos\theta_1\ddot{\theta}_1$$

$$\ddot{y}_1 = -l_{c1}\cos\theta_1\dot{\theta}_1^2 - l_{c1}\sin\theta_1\ddot{\theta}_1$$

$$\ddot{x}_2 = -l_1\sin\theta_1\dot{\theta}_1^2 + l_1\cos\theta_1\ddot{\theta}_1 - l_{c2}\sin(\theta_1+\theta_2)(\dot{\theta}_1+\dot{\theta}_2)^2 + l_{c2}\cos(\theta_1+\theta_2)(\ddot{\theta}_1+\ddot{\theta}_2)$$

$$\ddot{y}_2 = -l_1\cos\theta_1\dot{\theta}_1^2 - l_1\sin\theta_1\ddot{\theta}_1 - l_{c2}\cos(\theta_1+\theta_2)(\dot{\theta}_1+\dot{\theta}_2)^2 - l_{c2}\sin(\theta_1+\theta_2)(\ddot{\theta}_1+\ddot{\theta}_2) \tag{2.22}$$

For the ease of developing simulation program and system identification, the discrete form of the dynamic equations will be formulated. Using the previously defined Equation (2.19), the first order approximation of the biped for the data sampling can be expressed as ($h$ is the sampling rate):

$$q_1(n+1) = q_1(n) + hq_3(n)$$

$$q_2(n+1) = q_2(n) + hq_4(n)$$

$$q_3(n+1) = q_3(n) + \frac{h}{D}\Bigg[\delta(n)\tau_1(n) - (\delta(n) + \frac{\beta(n)}{2}\cos q_2(n))\tau_2(n)$$
$$+\left(\delta(n)(q_3(n)+q_4(n))^2 + \frac{\beta(n)}{2}q_3^2(n)\cos q_2(n)\right)\frac{\beta(n)}{2}\sin q_2(n)$$
$$-\left(\frac{\beta(n)}{2}m_2 l_{c2}\cos q_2(n)\sin(q_1(n)+q_2(n)) - \delta(n)(m_1 l_{c1} + m_2 l_1)\sin x_1(n)\right)g\Bigg]$$

$$q_4(n+1) = q_4(n) + \frac{h}{D}\Bigg[ -(\delta(n) + \frac{\beta(n)}{2}\cos q_2(n))\tau_1(n) + (\delta(n) + \beta(n)\cos q_2(n))\tau_2(n)$$
$$-\Bigg( (\delta(n) + \frac{\beta(n)}{2}\cos q_2(n))(q_3(n) + q_4(n))^2$$
$$+ q_3^2(n)(\alpha(n) - \delta(n) + \frac{\beta(n)}{2}\cos q_2(n)\Bigg)\frac{\beta(n)}{2}\sin q_2(n) \qquad (2.23)$$
$$+\Bigg( -(\delta(n) + \frac{\beta(n)}{2}\cos q_2(n))(m_1 l_{c1} + m_2 l_1)\sin q_1(n)$$
$$+ (\alpha(n) - \delta(n) + \frac{\beta(n)}{2}\cos q_2(n))m_2 l_{c2}\sin(q_1(n) + q_2(n))\Bigg) g\Bigg]$$

where $D = m_1 m_2 l_{c1}^2 l_{c2}^2 + m_1 l_{c1}^2 I_2 + m_2 l_{c2}^2 I_1 + m_2^2 l_{c2}^2 l_1^2 + m_2 l_1^2 I_1 + I_1 I_2 - m_2^2 l_{c2}^2 l_1^2 \cos^2 q_2(n)$

The foot-link is not fixed on the ground, but is required to be stationary. Thus, the two joint torques are limited by three constraints (Yang and Wu 2006b): the gravity constraint verifies that the foot-link does not lift from the ground; the friction constraint ensures the foot does not slip and the Center of Pressure (COP) constraint requires that the COP reside within the boundary of the support.

The constraints can be expressed as the following:

a. **Gravity constraint:** The gravity constraint ensures that the biped's feet do not lift from the ground:

$$F_{gy} \geq 0 \qquad (2.24)$$

b. **Friction constraint:** The friction constraint ensures that the biped's feet do not slide on the ground:

$$\left|F_{gx}\right| \leq \mu F_{gy} \qquad (2.25)$$

c. **Center of Pressure Constraint:** The COP constraint requires the COP reside within the

boundary of support.

$$x_{cop} = L_a - \frac{L_b F_{gx} + \tau_1 - L_c m_f g}{F_{gy}} \tag{2.26}$$

$$0 \le x_{cop} \le L_f \tag{2.27}$$

The 4-dimensional, state-space model Equation (2.23) leads to four Lyapunov exponents. The signs of the Lyapunov exponents provide qualitative information about the system stability. The linearization of the model of Equation (2.23) is:

$$\dot{q}_j(n) = J_{ji}(n) q_i(n-1) \qquad (i,j=1,2,3,4) \tag{2.28}$$

where the system Jacobian $J$ is a $4 \times 4$ matrix.

In this thesis, RBFNN is used to identify the discrete-time nonlinear biped balance system. The RBFNN model is obtained by having a network with four input nodes to the state $q(n) = [\, q_1(n) , q_2(n) , q_3(n) , q_4(n) \,]$. The output of the network will be $\hat{q}(n) = [\, \hat{q}_1(n) , \hat{q}_2(n) , \hat{q}_3(n) , \hat{q}_4(n) \,]$. The control law is embedded in the neural structure. The gradient descent method with momentum is often too slow for practical problems. For better performance of system identification, both supervised and unsupervised algorithms are employed to train the RBFNN.

First, 100 sample data, which are uniformly distributed in the state space, are selected to initialize the radial basis function centers and the weight parameters. That means the RBFNN adopts 100 hidden nodes for each output structure. Then, the actual outputs of the plant at each instance are used as teaching signals and the problem is to adapt the network

parameters so as to minimize the generalized error. This will be achieved using the block diagram shown in Figure 2.7.

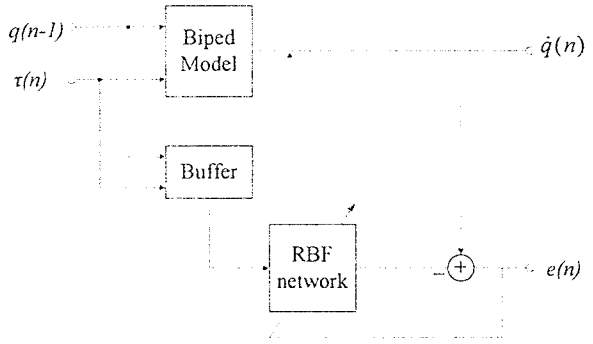


Figure 2.7 Identification of biped balance system

Let $e_k$ *(n)* denote the error between the system output $\dot{q}_k(n)$ and the RBFNN output $\hat{\dot{q}}_k(n)$ at time *n*.

$$e_k(n) = \dot{q}_k(n) - \hat{\dot{q}}_k(n), \quad k=1,2,3,4 \tag{2.29}$$

The performance index function of the RBF network at time *n* is defined as

$$CF_k(n) = \frac{1}{2} e_k^2(n) \tag{2.30}$$

Note that during the learning or adaptation process, the RBFNNs use the system state $\dot{q}(n)$ rather than the network state $\hat{\dot{q}}(n)$. However, once the learning process is terminated, the RBFNNs are independent of the system.

Using the RBFNNs, the system Jacobians are derived as follows:

$$J_{ki} = \frac{\partial \dot{q}_k(n+1)}{\partial q_i(n)} \approx \frac{\partial \hat{\dot{q}}_k(n+1)}{\partial q_i(n)} = \sum_{j=1}^{L} w_{kj}\phi_{kj} \frac{c_{kji} - q_i(n)}{b_{kj.}^2} \tag{2.31}$$

In Chapters 3 and 4, this method is used for the calculation of Lyapunov exponents. To

verify the effectiveness of the proposed method, the Lyapunov exponents based on the neural Jacobians are compared to the ones based on the actual Jacobians derived from the mathematical model.

# Chapter 3

# LQR Balance Control

## 3.1 Introduction

The design of low energy-cost control algorithms is highly desirable for regulating biped locomotion.

In this chapter, a classical state feedback control using the Linear Quadratic Regulator (LQR) technique is proposed to stabilize the standing biped. The LQR problem is equivalent to a dynamic optimization problem for linear differential equations. Its significance for control theory was first discussed fully by Kalman in 1960 (Kalman 1960). One of its main applications is to steer the solution of the underlying linear differential equation to a desired reference trajectory with minimal cost given the dynamic equations. Thus, LQR feedback can be used to improve energy efficiency of the biped balance system.

Since the upright posture of a biped is inherently unstable and the LQR control law is based on the linearized biped model, the stability of such a nonlinear control system is analyzed using the concept of Lyapunov exponents. The Lyapunov exponents are calculated based on the mathematical model of the biped system. The Jacobians determined using both the mathematical model and the neural model of the biped system are compared, to demonstrate the effectiveness of RBFNN identification for the determination of Jacobians. Part of the stability region of the proposed control system is also determined using Lyapunov exponents.

The first objective of this chapter is to design an optimal control to minimize the torque outputs and to keep the biped at the upright position. The constraints between the biped feet and the ground are examined to ensure their satisfaction.

The second objective is to analyze the stability of the proposed controller using the concept of Lyapunov exponents. To show the capability of the neural Jacobians for the calculation of Lyapunov exponents, the results of Lyapunov exponents based on the neural Jacobians derived from the RBFNN model are compared to the results based on the actual Jacobians derived from the mathematical model.

## 3.2 Linear Quadratic Regulator (LQR) Theory

The approach to the design of a LQR consists of the formulation of an optimal control problem on a semi-infinite time interval. It turns out that the solution to the optimal

control problem comes in the form of a linear state law that is guaranteed to produce an asymptotically stable closed-loop system (Goodwin *et al.*, 2000). Using LQR theory, it has been established that for a controllable linear time-invariant system, a set of optimal feedback gains may be found which minimizes a quadratic index and makes a closed-loop system stable. A system can be expressed in a state variable form as

$$\dot{x} = Ax + Bu \tag{3.1}$$

with $x \in R^n$, $u \in R^n$. We assume here that all the states are measurable and seek to find a state feedback control

$$u = -Kx \tag{3.2}$$

where $K$ is a constant matrix.

To design an optimal state-feedback controller, we define the performance index

$$PI = \frac{1}{2}\int_0^\infty (x^T Qx + u^T Ru)dt \tag{3.3}$$

Substituting Equation (3.2) into Equation (3.3) yields

$$PI = \frac{1}{2}\int_0^\infty x^T (Q + K^T RK)xdt \tag{3.4}$$

The objective in optimal design is to select the $K$ to minimize the performance index $PI$. It should be noted that both the state $x$ and the control input $u$ are weighted in $PI$, so that if $PI$ is low, neither $x$ nor $u$ can be too large. If $PI$ is minimized, and since it is an infinite integral of $x$, this implies that $x$ goes to zero as $t$ goes to infinity. This in turn guarantees that the linear system is stable.

The weight matrices $Q$ (a $n \times n$ matrix) and $R$ (a $m \times m$ matrix) are the most important components in LQR optimization. The performance of $Q$ and $R$ determines the output performance of the system. Commonly, a trial-and-error method has been used to construct the matrices $Q$ and $R$. One should select $Q$ to be positive semi-definite, and $R$ to be positive definite. This means that the scalar quantity $x^T Qx$ is always positive or zero, at each time $t$ for all functions $x$, and the scalar quantity $u^T Ru$ is always positive at each time $t$ for all values of $u$ except zero. This guarantees that $PI$ is well-defined. In terms of eigenvalues, the eigenvalues of $Q$ should be non-negative, while those of $R$ should be positive. If both matrices are selected diagonal, this means that all the entries of $R$ must be positive while those of $Q$ should be positive, with possibly some zeros on its diagonal. Note that $R$ is invertible.

Since the plant is linear and the performance index $PI$ is quadratic, the problem of determining the $K$ to minimize $PI$ is called the Linear Quadratic Regulator (LQR). The word "regulator" refers to the fact that the function of this feedback is to regulate the states to zero. This is in contrast to the tracking problems, where the objective is to make the output follow a prescribed (usually nonzero) reference command.

To find the optimal feedback $K$, we proceed as follows. Suppose there exists a constant matrix $P$ such that

$$\frac{d}{dt}(x^T Px) = -x^T (Q + K^T RK)x \tag{3.5}$$

Then, substituting Equation (3.5) into Equation (3.4) yields

$$PI = -\frac{1}{2}\int_0^\infty \frac{d}{dt}(x^T Px)dt = \frac{1}{2}x^T(0)Px(0) \tag{3.6}$$

where we assume that $x$ goes to zero as time $t$ goes to infinity. Equation (3.6) indicates that $PI$ is now independent of $K$. It is a constant that only depends on the auxiliary matrix $P$, and the initial conditions.

Now, we can find a matrix $K$ so that assumption (3.5) does indeed hold. To accomplish this, differentiate (3.5) and then substitute the state Equation (3.1) and control Equation (3.2) into Equation (3.5), yielding

$$\dot{x}^T Px + x^T P\dot{x} + x^T Qx + x^T K^T RKx = 0 \tag{3.7}$$

$$x^T(A-BK)^T Px + x^T P(A-BK)x + x^T Qx + x^T K^T RKx = 0 \tag{3.8}$$

$$x^T\left[(A-BK)^T P + P(A-BK) + Q + K^T RK\right]x = 0 \tag{3.9}$$

Equation (3.9) has to hold for every $x$. Therefore, the term in square bracket must be equal to zero. Thus, we have

$$(A-BK)^T P + P(A-BK) + Q + K^T RK = 0 \tag{3.10}$$

$$A^T P + PA + Q + K^T RK - K^T B^T P - PBK = 0 \tag{3.11}$$

This is a matrix quadratic equation in the variable of $K$. One way to solve it is by completing the square. Though this procedure is a bit complicated for matrices, suppose we select

$$K = R^{-1}B^T P \tag{3.12}$$

Substituting Equation (3.12) into Equation (3.11) gives

$$A^T P + PA + Q + (R^{-1}B^T P)^T R(R^{-1}B^T P) - (R^{-1}B^T P)^T B^T P - PB(R^{-1}B^T P) = 0 \quad (3.13)$$

$$A^T P + PA + Q - PBR^{-1}B^T P = 0 \quad (3.14)$$

This result is of extreme importance in modern control theory. Equation (3.14) is known as the algebraic Riccati Equation (ARE). It is named after Count Riccati, an Italian who lived in the 19th century and used a similar equation in the study of heat flow. It is a matrix quadratic equation that can be solved for the auxiliary matrix $P$ given $(A,B,Q,R)$. The optimal state feedback gain is given by Equation (3.12). The minimal value of the $PI$ using this gain is given by Equation (3.6), which only depends on the initial condition. This means that the energy cost $PI$ of LQR control using the gains in Equation (3.12) can be computed from the initial conditions before the control is ever applied to the system.

The design procedure for finding the LQR feedback $K$ is:

- Select design parameter matrices Q and R.
- Solve the algebraic Riccati equation for P
- Find the state feedback gain using $K = R^{-1}B^T P$

There are well-developed numerical procedures for solving the ARE. The MATLAB routine that performs this is named *lqr(A,B,Q,R)*, which is used in this work.

## 3.3 LQR Balance Control Design for Biped Standing

In this chapter, a biped balance system is designed using LQR techniques. In order to obtain the LQ parameters, the biped model is required to be linearized about the equilibrium point, which is defined as the upright position of the link 1 and link 2. Therefore, the system is linearized about the point ($q_1 = 0, q_2 = 0, q_3 = 0, q_4 = 0$) with $[\tau_1, \tau_2] = [0,0]$. Using common mathematical linearization techniques, the nonlinear sine and cosine terms can be evaluated into linear terms. This is shown in Table 3.1.

| Nonlinear | $\sin q_1$ | $\sin q_2$ | $\cos q_2$ | $\sin(q_1 + q_2)$ |
|---|---|---|---|---|
| Linear | $q_1$ | $q_2$ | 1 | $q_1 + q_2$ |

Table 3.1 Linearizing function table

Replacing the nonlinear terms of the state-space equation with the linear terms derived in Table 3.1, the linearized state-space equations can then be formulated. The complete linearized state-space equations are shown:

$$\dot{q}_1 = q_3$$

$$\dot{q}_2 = q_4$$

$$\dot{q}_3 = \left[ \delta\tau_1 - (\delta + \frac{\beta}{2})\tau_2 + \left( \delta(q_3 + q_4)^2 + \frac{\beta}{2} q_3^2 \right) \frac{\beta}{2} q_2 \right.$$
$$\left. - \left( \frac{\beta}{2} m_2 l_{c2} (q_1 + q_2) - \delta(m_1 l_{c1} + m_2 l_1) q_1 \right) g \right] / D'$$

$$\dot{q}_4 = \Big[ -(\alpha + \frac{\beta}{2})\tau_1 + (\alpha + \beta)\tau_2$$
$$-\frac{\beta}{2} q_2 \Big( (\delta + \frac{\beta}{2})(q_3 + q_4)^2 + (\alpha - \delta + \frac{\beta}{2}) q_3^2 \Big) \qquad (3.15)$$
$$+ \Big( -(\delta + \frac{\beta}{2})(m_1 l_{c1} + m_2 l_1) q_1 + (\alpha - \delta + \frac{\beta}{2}) m_2 l_{c2} (q_1 + q_2) \Big) g \Big] / D'$$

where $D' = m_1 m_2 l_{c1}^2 l_{c2}^2 + m_1 l_{c1}^2 I_2 + m_2 l_{c2}^2 I_1 + m_2^2 l_{c2}^2 l_1^2 + m_2 l_1^2 I_1 + I_1 I_2 - m_2^2 l_{c2}^2 l_1^2$.

The matrices $A$ and $B$ of LQR as shown in Equation (3.1) are determined by the follow equations:

$$A_{ij} = \frac{\partial \dot{q}_i}{\partial q_j}, \ (i, j = 1,2,...,4)$$

$$B_{ij} = \frac{\partial \dot{q}_i}{\partial \tau_j}, \ (i = 1,2,...,4, \ j = 1,2) \qquad (3.16)$$

The physical parameters of the biped model are taken from the reference (Yang and Wu 2006) as shown in Table 3.2.

| $m_1$ (kg) | $m_2$ (kg) | $m_f$ (kg) | $l_1$ (m) | $l_2$ (m) | $L_f$ (m) | $L_a$ (m) | $L_b$ (m) | $L_c$ (m) | $\mu$ |
|---|---|---|---|---|---|---|---|---|---|
| 48.72 | 28.96 | 2.32 | 0.998 | 0.712 | 0.27 | 0.05 | 0.07 | 0.085 | 0.5 |

Table 3.2: Biped Model Parameters

By using the above parameters and Equations (3.15) and (3.16), the numerical values of the A and B matrices for the biped model are

$$A = \begin{bmatrix} 0 & 0 & 1 & 0 \\ 0 & 0 & 0 & 1 \\ 13.2290 & -9.0929 & 0 & 0 \\ -20.3763 & 48.8780 & 0 & 0 \end{bmatrix}$$

$$B = \begin{bmatrix} 0 & 0 \\ 0 & 0 \\ 0.0428 & -0.1327 \\ -0.1327 & 0.6159 \end{bmatrix} \tag{3.17}$$

The $Q$ and $R$ designed for the linearized biped system are chosen based on trial and error as shown below

$$Q = \begin{bmatrix} 1000 & -500 & 0 & 0 \\ -500 & 1000 & 0 & 0 \\ 0 & 0 & 1000 & -500 \\ 0 & 0 & -500 & 1000 \end{bmatrix}$$

$$R = \begin{bmatrix} 1000 & 0 \\ 0 & 1000 \end{bmatrix} \tag{3.18}$$

Matlab was used to determine the corresponding state-space feedback gains given by

$$K_{LQR} = \begin{bmatrix} 1059.8 & 63.1 & 344.5 & 53.7 \\ 273.3 & 206.6 & 106.5 & 43.9 \end{bmatrix} \tag{3.19}$$

The initial condition used to test this and other balance controllers was $[q_1, q_2, q_3, q_4]$=[-0.05rad,0.03rad,0.05rad/s,-0.03rad/s]. Figure 3.1 (a) and (b) show the simulated angular displacements and control torques using LQR control. We can see that the proposed controller successfully stabilized the biped at the upright posture within 2.5 seconds. The control performance for other initial conditions was also tested and the results are similar. Figure 3.2 shows the horizontal and vertical ground reaction forces. The positive vertical ground reaction force $F_{gy}$ ensures the support foot is in contact with the ground. Figure 3.3(a) shows the horizontal ground reaction force and the upper and

lower bounds of the friction. The horizontal ground reaction force $F_{gx}$ is lower than the maximum static friction ($-\mu F_{gy}$ and $\mu F_{gy}$), which indicates the foot-link does not slip. Figure 3.3(b) shows the locations of the center of pressure (COP) and their upper and lower bounds. The location of the center of pressure $X_{COP}$ resides within the contact surface between the foot-link and the ground indicating that the foot-link does not rotate about either its toe or its heel. The above results illustrate that the proposed LQR control can keep the foot stationary with the given initial condition.

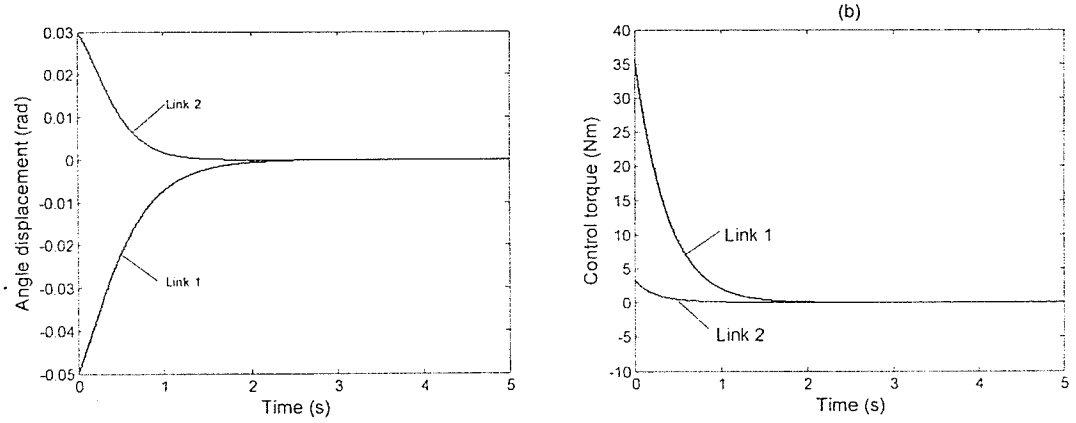


Figure 3.1 Simulation results using LQR control:
(a) angular displacements and (b) control torques.

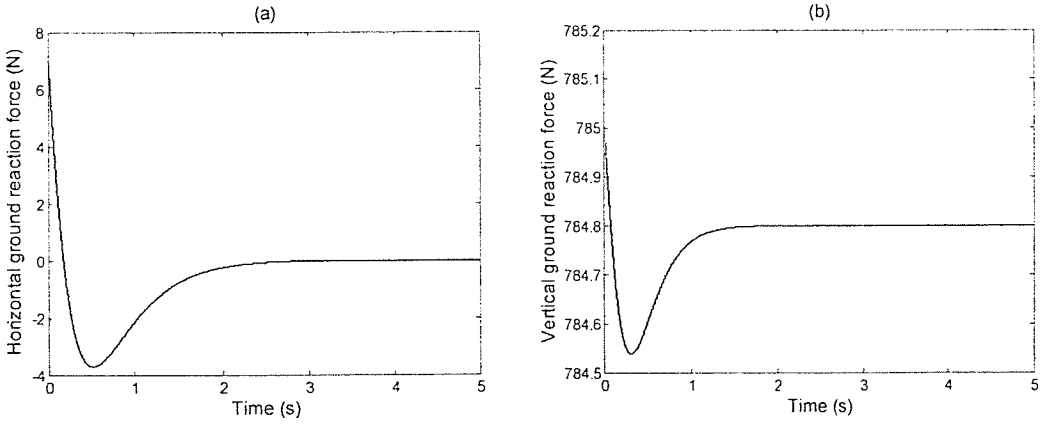


Figure 3.2 The ground reaction forces of the LQR control system (a) the horizontal ground reaction force and (b) the vertical ground reaction force

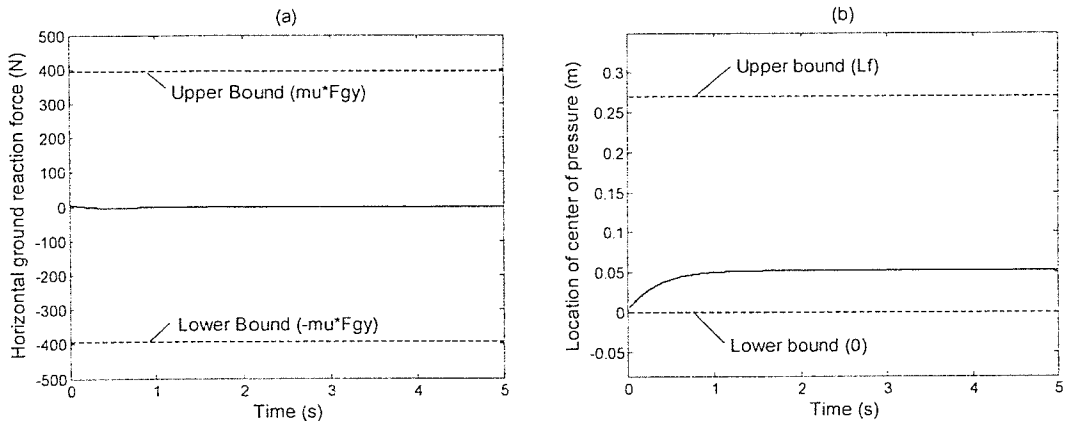


Figure 3.3 The constraints between the biped foot-link and the ground (a) the friction constraint and (b) the center of pressure constraint

## 3.4 Stability Analysis

Since the LQR control law is designed for the linearized system, there is no guarantee that it will work well when implemented on the nonlinear system. This is particularly true because the nonlinear system is not restricted close to the upright position. However, most previous works failed to provide the stability analysis of the nonlinear control systems due to system complexities. In this section, Lyapunov exponents are employed to analyze the stability of the LQR controller for the nonlinear biped system.

A neural approach to derive system Jacobians from RBFNN model is proposed for the calculation of Lyapunov exponents. The method can be used to analyze the stability of unknown systems. The biped balance system based on LQR control is used to demonstrate the effectiveness of the proposed neural method.

To adequately test the quality of the neural model (the procedure for developing the neural

model has been detailed in Chapter 2), the numerical Jacobians derived from the neural model using Equation (2.31) are plotted, to compare with the actual Jacobians derived from the mathematical model with the same initial condition $[q_1, q_2, q_3, q_4]$= [-0.05*rad*, 0.03*rad*, 0.05*rad/s*, -0.03*rad/s*]. In the first rows of Figures 3.4(a)-3.4(p), the solid lines are the actual Jacobians $J_{ij} = \frac{\partial \dot{q}_i}{\partial q_j}$ ($i,j$=1,2,3,4) determined from the mathematical model, and the dashed lines are the neural Jacobians $\hat{J}_{ij} = \frac{\partial \hat{\dot{q}}_i}{\partial q_j}$ ($i,j$=1,2,3,4) determined from the RBFNN model. The second rows in Figures 3.4(a)-3.4(p) show the absolute errors between the neural Jacobians and actual Jacobians (note that since some elements of the Jacobians are zero, the absolute errors are presented). After the biped is stabilized at the upright posture, all of the Jacobians become constants. The largest absolute error is less than 0.06. From these results, we can see that the neural model based on RBFNN identification is accurate to determine the actual Jacobians of the proposed biped balance system.

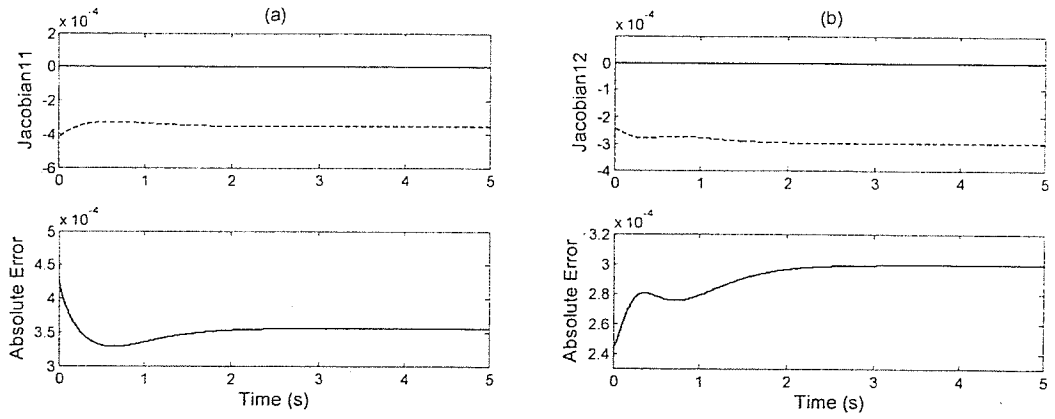

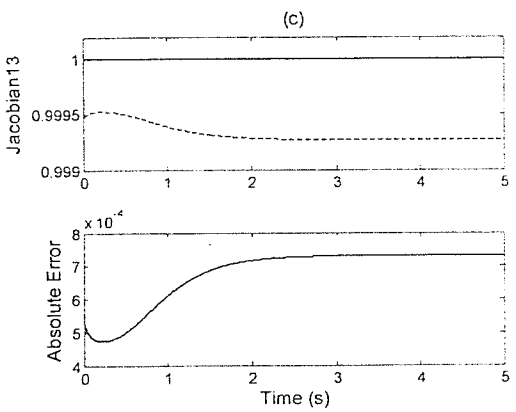
(c)
Jacobian13
Absolute Error
x 10^-4
Time (s)

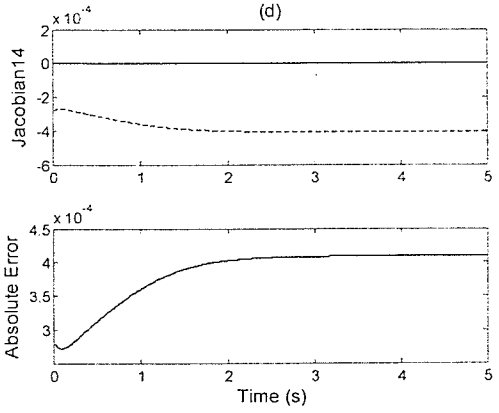
(d)
Jacobian14
Absolute Error
x 10^-4
Time (s)

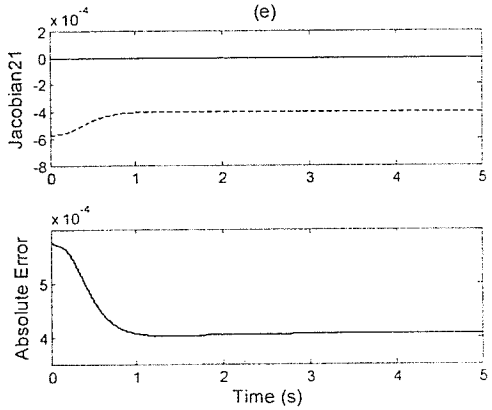
(e)
Jacobian21
Absolute Error
x 10^-4
Time (s)

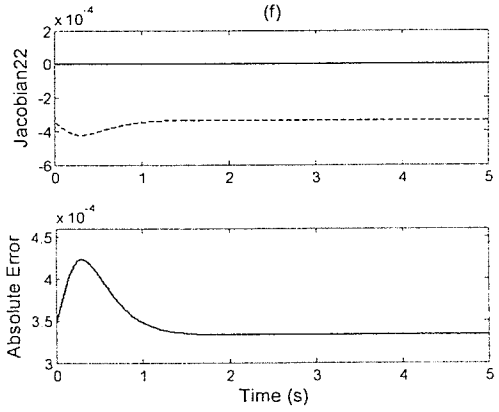
(f)
Jacobian22
Absolute Error
x 10^-4
Time (s)

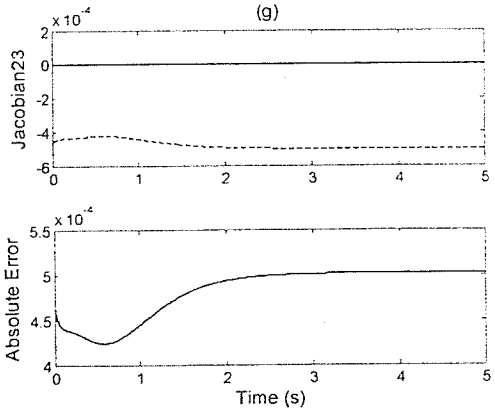
(g)
Jacobian23
Absolute Error
x 10^-4
Time (s)

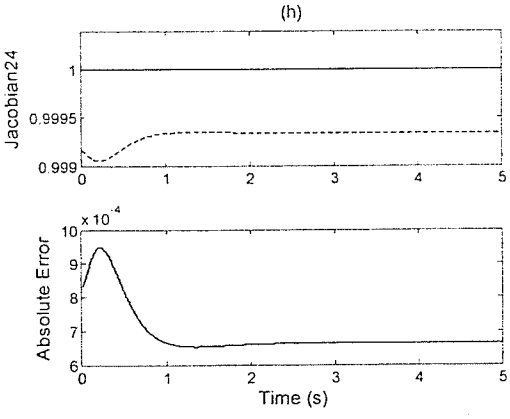
(h)
Jacobian24
Absolute Error
x 10^-4
Time (s)

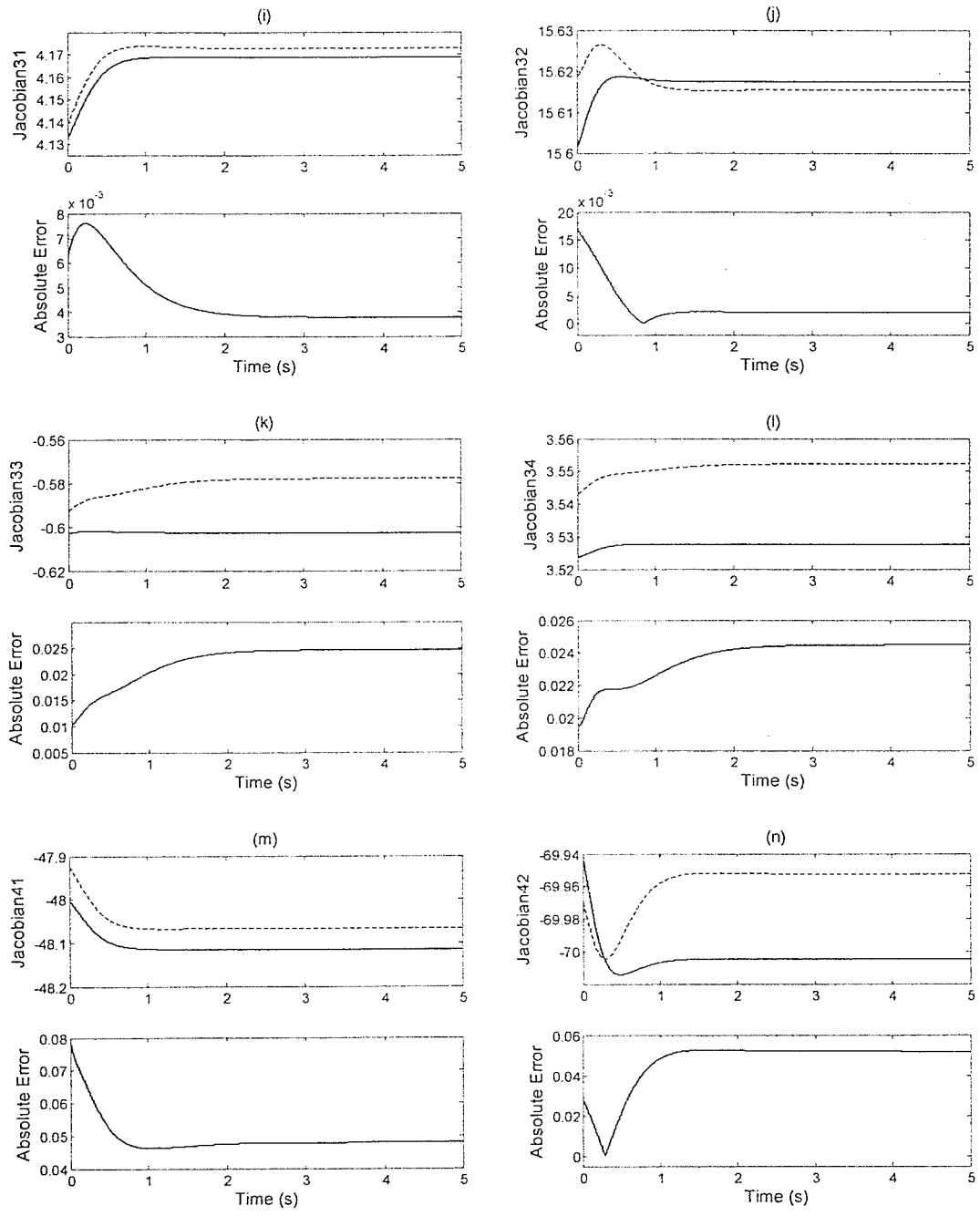
(i)
Jacobian31
4.17
4.16
4.15
4.14
4.13
0 1 2 3 4 5
x 10^-3
Absolute Error
8
7
6
5
4
3
0 1 2 3 4 5
Time (s)
(j)
Jacobian32
15.63
15.62
15.61
15.6
0 1 2 3 4 5
x 10^-3
Absolute Error
20
15
10
5
0
0 1 2 3 4 5
Time (s)
(k)
Jacobian33
-0.56
-0.58
-0.6
-0.62
0 1 2 3 4 5
Absolute Error
0.025
0.02
0.015
0.01
0.005
0 1 2 3 4 5
Time (s)
(l)
Jacobian34
3.56
3.55
3.54
3.53
3.52
0 1 2 3 4 5
Absolute Error
0.026
0.024
0.022
0.02
0.018
0 1 2 3 4 5
Time (s)
(m)
Jacobian41
-47.9
-48
-48.1
-48.2
0 1 2 3 4 5
Absolute Error
0.08
0.07
0.06
0.05
0.04
0 1 2 3 4 5
Time (s)
(n)
Jacobian42
-69.94
-69.96
-69.98
-70
0 1 2 3 4 5
Absolute Error
0.06
0.04
0.02
0
0 1 2 3 4 5
Time (s)

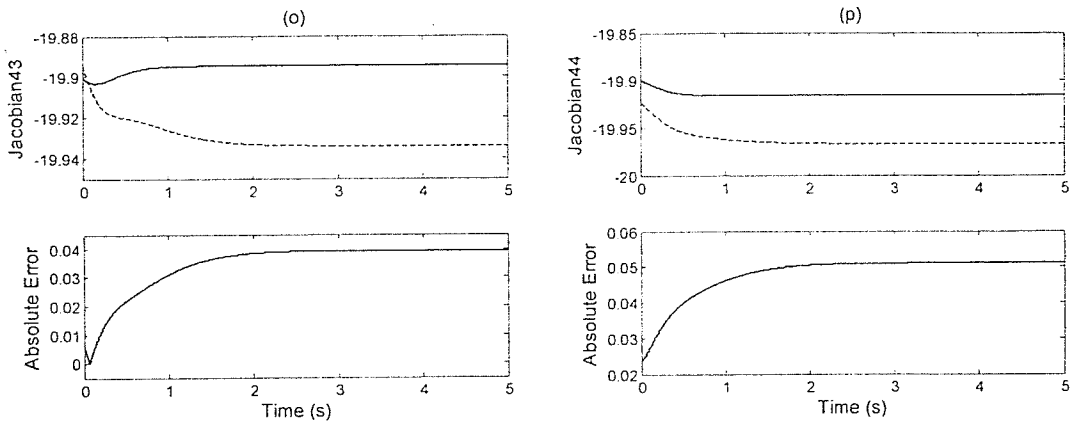


Figure 3.4 The actual and neural Jacobians of the LQR control system: the first rows show the actual Jacobians (solid lines) and the neural Jacobians (dashed lines), the second rows show the absolute errors between the above two Jacobians.

Four Lyapunov exponents for the LQR controlled biped system during standing as shown in Equation (2.7) were calculated. Stability analysis investigates the long-term behavior of motion under the influence of disturbance in the initial states. The four Lyapunov exponents in 100 seconds are shown in Figure 3.5. In the first rows of Figures 3.5(a)-3.5(d), the Lyapunov exponents based on the neural Jacobians (dashed lines) are compared to the respective exponents based on the actual Jacobians (solid lines). The second rows of Figures 3.5(a)-3.5(d) measure the relative errors of the Lyapunov exponents based on the neural Jacobians. The low relative errors illustrate that the approach to derive Jacobians from the RBFNN model of the LQR balance system is effective for the calculation of Lyapunov exponents. After 100 seconds, since the nonlinear term of Equation (2.23) disappeared; the Lyapunov exponents converge to constants which are listed in Table 3.3. All of the four Lyapunov exponents are negative indicating that the LQR control system is exponentially stable about the equilibrium point (the biped upright posture).

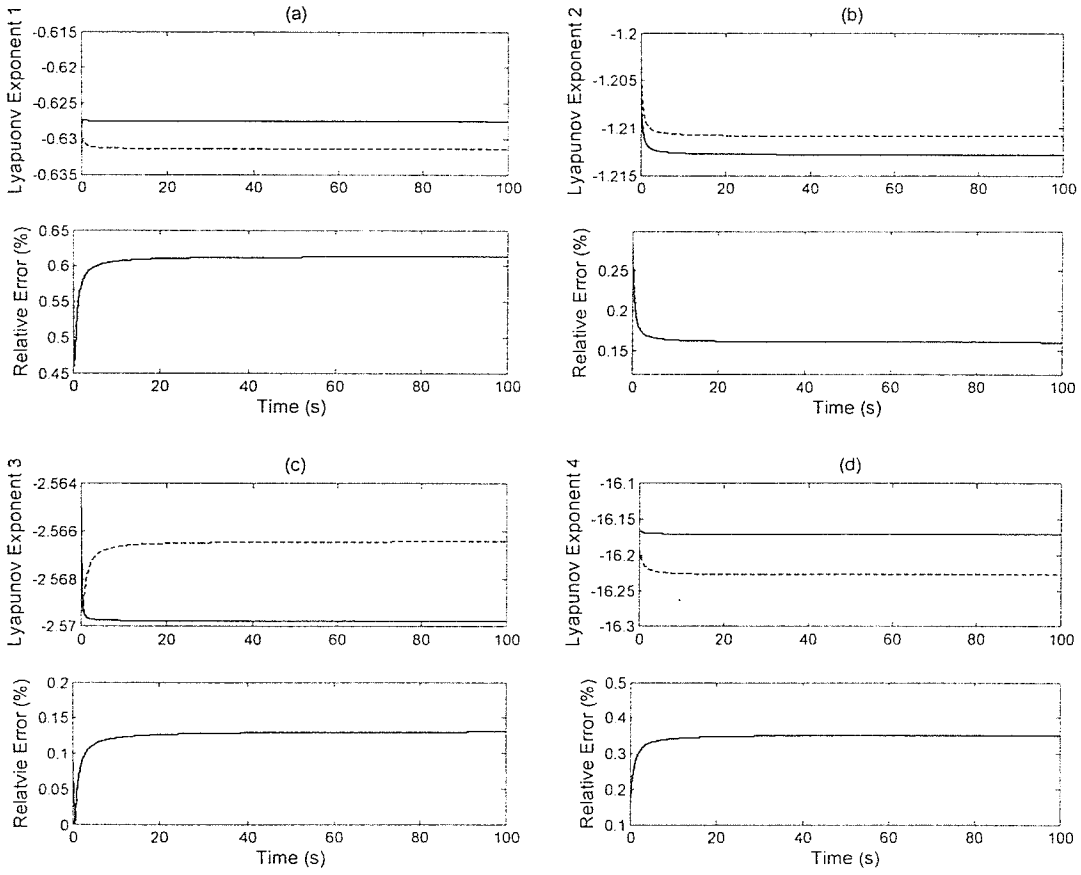


Figure 3.5 The Lyapunov exponents calculated based on the actual (solid lines) and neural (dashed lines) models of the LQR control system: (a) largest Lyapunov exponent (LE) (b) second LE (c) third LE (d) fourth LE.

| Lyapunov exponents (LE) | 1st LE | 2nd LE | 3rd LE | 4th LE |
|---|---|---|---|---|
| Mathematical model | -0.6276 | -1.2127 | -2.5698 | -16.1701 |
| Neural model | -0.6314 | -1.2107 | -2.5666 | -16.2254 |
| Relative error | 0.61% | 0.16% | 0.12% | 0.34% |

Table 3.3 The Lyapunov exponents and their relative errors after 100 seconds

Although the Lyapunov exponents are calculated using one trajectory, they remain the same value within the same stability region. The determination of the stability region is an

important part of the stability analysis. To determine the stability region, the algorithm developed by Nusse and Yorke (1998) is adapted, where the region of interest is first divided into grid boxes. The grid box at the origin of the state-space (also called center box) contains the stable equilibrium point.

Next, the size of neighboring grid boxes is chosen and the Lyapunov exponents are calculated using the initial states from each neighboring box. If the same convergent and negative exponents are obtained, the neighboring grid box belongs to the stability region. To find the stability region of the proposed LQR balance system, six regions in the phase plane are tested:

$$\Gamma_1 = \{q_1 \in [-1.5,1.5]rad, q_2 \in [-1.5,1.5]rad, q_3 = 0rad/s, q_4 = 0rad/s\}$$

$$\Gamma_2 = \{q_1 \in [-1.5,1.5]rad, q_2 = 0rad, q_3 \in [-1.5,1.5]rad/s, q_4 = 0rad/s\}$$

$$\Gamma_3 = \{q_1 \in [-1.5,1.5]rad, q_2 = 0rad, q_3 = 0rad/s, q_4 \in [-1.5,1.5]rad/s\}$$

$$\Gamma_4 = \{q_1 = 0rad, q_2 \in [-1.5,1.5]rad, q_3 \in [-1.5,1.5]rad/s, q_4 = 0rad/s\}$$

$$\Gamma_5 = \{q_1 = 0rad, q_2 \in [-1.5,1.5]rad, q_3 = 0rad/s, q_4 \in [-1.5,1.5]rad/s\}$$

$$\Gamma_5 = \{q_1 = 0rad, q_2 = 0rad, q_3 \in [-1.5,1.5]rad/s, q_4 \in [-1.5,1.5]rad/s\} \quad (3.20)$$

Each region is divided into grid boxes with the size of 0.01rad, 0.01rad, 0.01rad/s and 0.01rad/sec for $q_1$, $q_2$, $q_3$ and $q_4$, respectively. Figure 3.6 shows the stability region (grey color) which is determined by the largest Lyapunov exponent. In the above stability region, all of the largest Lyapunov exponents are negative and the mean value is -0.6313 with a deviation of $1.54\times10^{-4}$.

Note that, these regions are only part of the stability region and not necessarily the entire stability region. Finding the entire stability region of the proposed balance system is important, but it is out of the scope of this work.

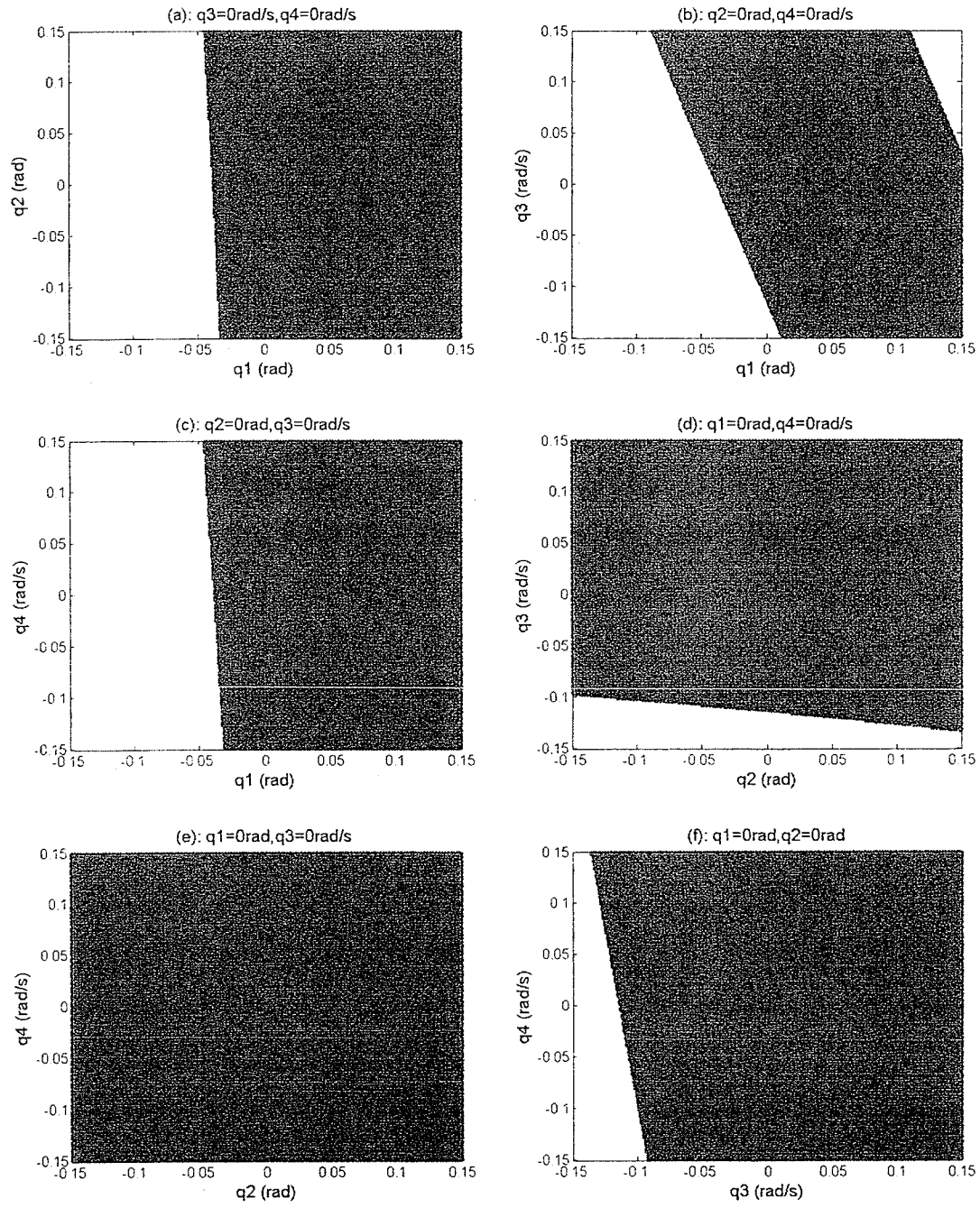


Figure 3.6 Part of the stability region of the LQR balance control for the biped

An objective of this chapter is to develop an energy-efficient control system to maintain the biped standing. A LQR feedback is employed for optimal control. The limitation is the constraints between the biped feet and the ground, which may not be satisfied during biped balancing. Thus, a GA-based PD control satisfying the above constraints will be introduced in the next chapter.

Another objective of this chapter is to analyze the stability of LQR control using the concept of Lyapunov exponents. The results indicate that the LQR biped control system is stable about the upright posture in the determined stability region.

In summary, a LQR controller is designed to balance a biped in the upright posture during standing. The stability is analyzed using the concept of Lyapunov exponents. The approach to calculate Lyapunov exponents based on RBFNN models is verified. Further, the RBFNN models show great capability of analyzing the stability of nonlinear control systems.

# Chapter 4

# GA-based PD Balance Control

## 4.1 Introduction

The design of balance control laws for standing bipeds is a challenging problem since the constraints between the biped feet and the ground (Equations 2.22-2.25) have significant effects on preventing a standing biped from falling over.

This chapter proposes a Genetic Algorithm (GA)-based PD control, which can guarantee the satisfaction of the constraints between the feet and the ground as well as minimize energy consumption of torque output. Due to the local optimization of PD gains according to the initial conditions, the stability of the proposed controller should be analyzed. However, in most of these approaches related to optimal control, stability has not been investigated systematically. In this work, the stability is verified through the concept of Lyapunov exponents and part of the stability region is determined as well.

The first objective of this chapter is to develop a biped balance system with the satisfaction of the constraints between the feet and the ground. The second objective is to analyze the stability of the proposed balance system using the concept of Lyapunov exponents.

To show the capability of the neural Jacobians for the calculation of Lyapunov exponents, the results of the Lyapunov exponents based on the neural Jacobians derived from the RBFNN model, are compared to those based on the actual Jacobians derived from the mathematical model. It demonstrates the capability of the proposed approach in calculating Jacobians using neural models for determining Lyapunov exponents.

## 4.2 Genetic Algorithm (GA)

Genetic algorithms (GAs) are robust, stochastic and heuristic search algorithms and optimization methods based on biological reproduction processes. Artificial reproduction schemes were first developed in the 70's (Holland, 1992) and were more extended during the 80's (Goldberg, 1989). The search area for the GAs is very wide and usually converges to a point near the global optimum. A GA is based on representing a solution to the problem as a chromosome. The GA creates a population of solutions and then applies genetic operators to "evolve" the solutions, in order to find the best one(s).

The following outline summarizes how the GA works:

Step 1: The algorithm begins by creating a random initial population as a starting point for the search.

Step 2: The algorithm then creates a sequence of new populations. At each step, the algorithm uses the individuals in the current generation to create the next population. To create the new population, the algorithm performs the following steps:

a. Score each member of the current population by computing its fitness value based on the cost function.

b. Select some individuals (called parents) in the population for reproduction based on the relative fitness of the individuals.

c. Choose some of the individuals in the current population that have lower fitness as elite. These elite individuals are passed on to the next population.

d. Produce children from the parents by means of a crossover and mutation operator. A crossover takes two parents and swaps parts of their genetic information to produce new chromosomes. A mutation operator produces new single parents in the population by randomly modifying some of the genes.

e. Replace the current population with the children to form the next generation.

Step 3: These processes are repeated until a satisfactory individual is found or a certain stop condition is met.

At each step, the GA uses the current population to create children that make up the next generation. The algorithm selects a group of individuals in the current population called parents, who contribute their genes, the entries of their vectors, to their children. The algorithm usually selects individuals that have better (lower) fitness values, as parents.

The GA creates three types of children for the next generation:

- Elite children are the individuals in the current generation with the best fitness values. These individuals automatically survive to the next generation.
- Crossover children are created by combining the vectors of a pair of parents. If the coding is chosen properly, two good parents produce good children.
- Mutation children are created by introducing random changes, or mutations, to a single parent. In real evolution, the genetic material can be changed randomly by erroneous reproduction or other deformations of genes. In GAs, mutation can be realized as a random deformation of the chromosomes with a certain probability. The positive effect is preservation of genetic diversity and avoidance of local minima.

Compared to traditional continuous optimization methods, such as Newton or gradient descent methods, the significant differences are as follow:

1. GAs manipulate coded versions of the problem parameters instead of the parameters themselves.
2. While almost all conventional methods search from a single point, GAs always operate on a whole population of points. This contributes a great deal to the robustness of GAs. It improves the chance of reaching the global optimum and, vice versa, reduces the risk of becoming trapped in a local stationary point.
3. Normal GAs do not use any auxiliary information about the objective function value such as derivatives. Therefore, they can be applied to any kind of continuous or

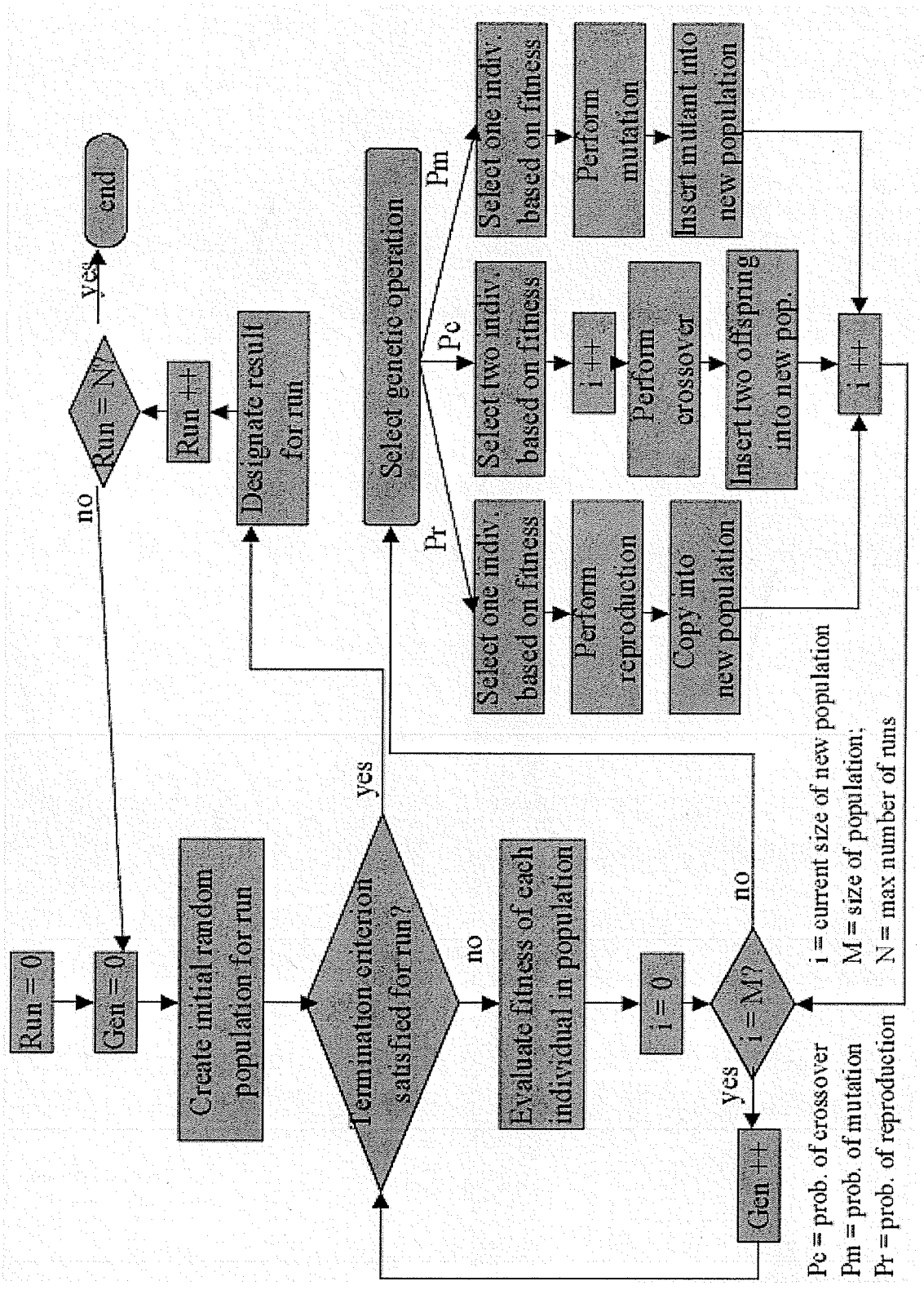


Figure 4.1 GA flow chart

discrete optimization problem. The only thing to be done is to specify a meaningful decoding function.

4. GAs use probabilistic transition operators while conventional methods for continuous optimization apply deterministic transition operators. More specifically, the way a new generation is computed from the actual one has some random components.

## 4.3 GA-based PD Balance Control Design for Biped Standing

In this chapter, a PD balance system is designed to stabilize the standing biped in an upright posture, shown in Equation 4.1. A GA is employed to tune the PD gains of the controllers for a given set of initial conditions. The aims of GA are to satisfy the constraints between the biped feet and the ground, to minimize energy consumption and keep the biped in an upright posture.

$$\begin{cases} \tau_1 = -k_{P1}q_1 - k_{D1}q_3 \\ \tau_2 = -k_{P2}q_2 - k_{D2}q_4 \end{cases} \tag{4.1}$$

It has been well-accepted that the energy to control the position of the biped is closely related to the integration of the square of the torque, with respect to time. Thus, minimizing the torque indicates minimizing the energy consumption. The cost function $J$ can be defined as follows:

$$J = \frac{1}{2}\left[ \int_0^{t_f} (C_1\tau_1^{\,2} + C_2\tau_1^{\,2} + C_3q_1^2 + C_4q_2^2 + C_5q_3^2 + C_6q_4^2)dt + \int_0^{t_f} C_{constraint}\,dt) \right] \tag{4.2}$$

$$C_{constraint} = \begin{cases} 0 & \text{if the constraints are satisfied.} \\ C_7 & \text{if the constraints are not satisfied.} \end{cases} \tag{4.3}$$

where $t_f$ is the final time instance and $C_j$ (j=1, 2, ..., 7) are the weighting coefficients. By

using different values for the weighting coefficients $C_j$, it is possible to tune the balance system to meet different criteria. In this work, the weighting coefficients are selected as $C_1$=0.001, $C_2$=0.001, $C_3$=50, $C_4$=50, $C_5$=10, $C_6$=10, $C_7$=1000. $C_{constraint}$ is the constraint function for satisfying the constraints between the biped foot-link and the ground in Equations (2.24)-(2.27).

For the optimization of the cost function, a real-valued GA (representing each chromosome as a real-valued number) is used because it has several advantages over a binary GA (representing each chromosome as a bit string). Programming is simple and the searching speed is improved since encoding and decoding the processes is not necessary. This is due to the one-to-one correspondence between a phenotype and a genotype. It is possible to define a very large domain and easy to deal with highly complex constraints. Many experiments comparing real-valued and binary GAs have proven that the real-valued generates better results in terms of the solution quality and computation time (Michalewich 1996).

The population size for the GA is set to 60, crossover probability is 0.8 and mutation probability is 0.01. The maximum number of generations is 100. The GA will terminate when a maximum number of generations has been produced or the value of the cost function does not improve for 10 consecutive generations. If the constraints are greater than $C_7$ or at $t_f$=5$s$ the biped is outside the upright region, $\{|q_1|<0.002,\ |q_2|<0.002,\ |q_3|<0.005,\ |q_4|<0.005\}$, GA will be considered to have failed to find the solution of PD gains.

The physical parameters of the biped model are shown in Table 3.2. In the simulation, the initial state is $q_1 = -0.05\ rad$, $q_2 = 0.03\ rad$, $q_3 = 0.05\ rad/s$ and $q_4 = -0.03\, rad/s$, the final time is $t_f$=5$s$ and the step size is $h$=0.01. Figure 4.2 shows the variation of the cost function $J$. We can see that the GA converges with 53 generations.

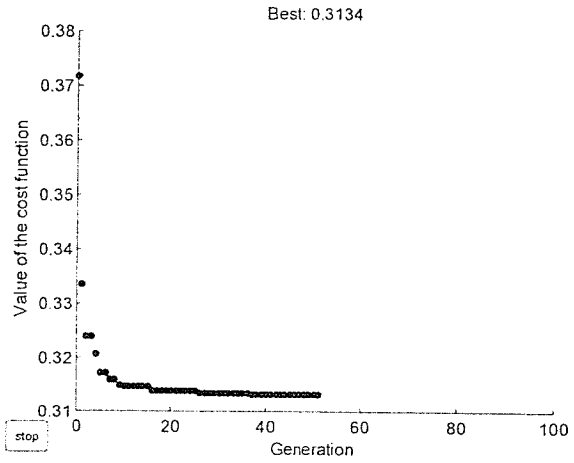


Figure 4.2 The variation of the cost function

The PD gains obtained by the GA are $K_{P1}$= 725.82, $K_{P2}$=236.21, $K_{D1}$= 171.75, and $K_{D2}$= 179.39. The value of the cost function (Equation 4.2) $J$ is 0.3134. Compared to the value of LQR control ($J$=0.4030) in Chapter 3 with the same initial condition, it is clear that GA-based PD control reduces the value of the cost function. This indicates that the energy consumed is reduced significantly. Figure 4.3(a) and (b) show the simulated angular displacements and control torques of the proposed controller. The biped approaches the upright posture within 3 seconds. Figure 4.4(a) and (b) show the ground reaction forces in horizontal and vertical directions. Figure 4.5(a) shows the horizontal ground reaction force and the upper and lower bounds of the static frictions. Figure 4.5(b) shows the

location of the COP and the bounds of the contact surface between the foot-link and the ground. From Figures 4.4 and 4.5, it can be easily observed that the satisfaction of the constraints between the feet and the ground is verified. The vertical ground reaction force $F_{gy}$ is always positive, as shown in Figure 4.4(b). The force in the horizontal direction $F_{gx}$ is always less than the maximum force of the static friction ($\mu F_{gy}$ and $-\mu F_{gy}$), as shown in Figure 4.5(a). The center of pressure in the horizontal direction is always inside the foot length as shown in Figure 4.5(b). It is concluded that the proposed control scheme can maintain the biped balance in an upright posture while keeping the foot stationary.

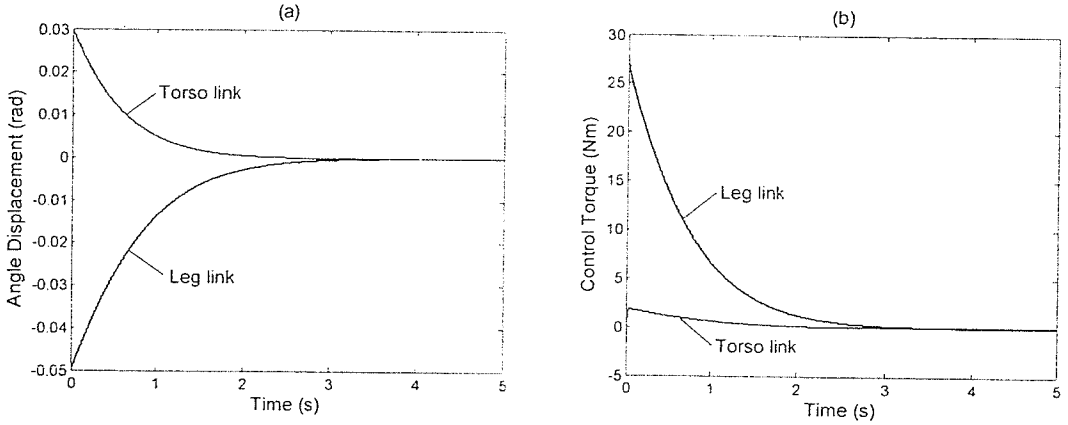


Figure 4.3 Simulation results using GA-based PD control
(a) angular displacements and (b) control torques

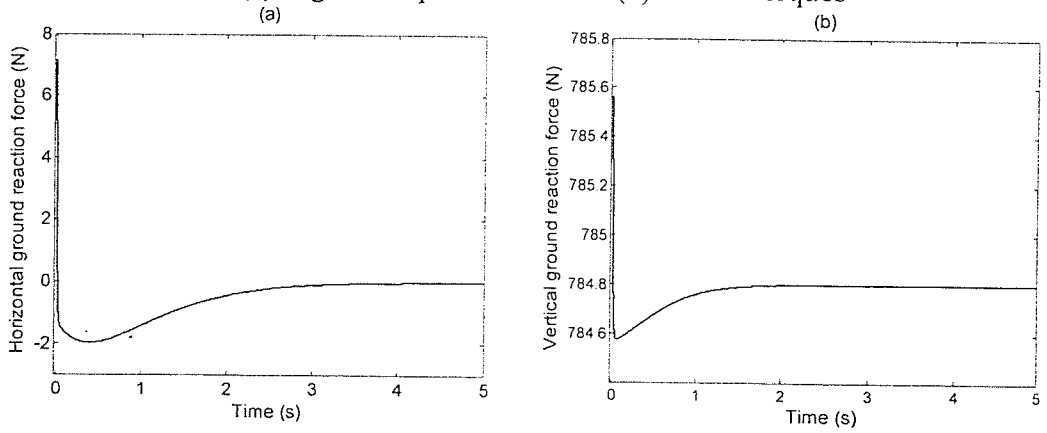


Figure 4.4 The ground reaction forces of the GA-based PD control system (a) the horizontal ground reaction force and (b) the vertical ground reaction force.

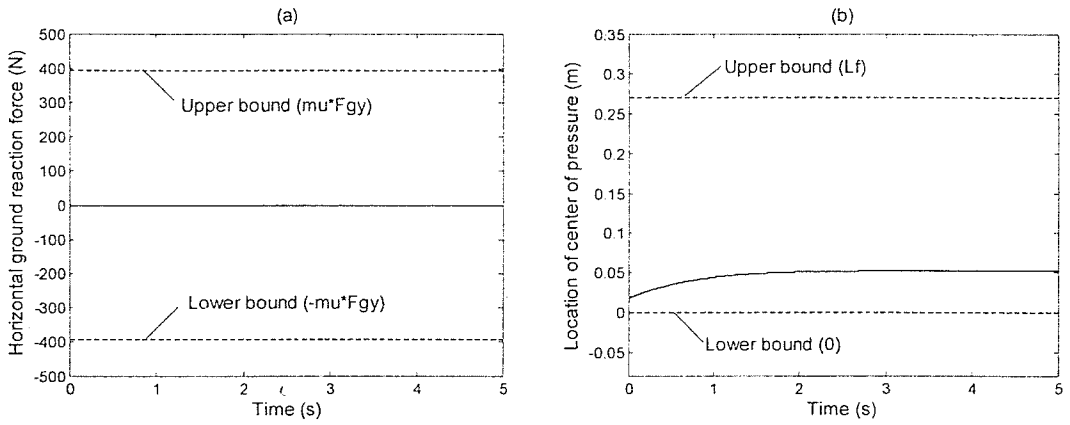


Figure 4.5 The constraints between the biped foot-link and the ground of the GA-based PD control (a) The friction constraint, (b) The COP constraint

## 4.5 Stability Analysis

The upright posture of biped standing has an unstable equilibrium point. For the proposed GA-based PD control, the PD gains are optimized locally, according to specific initial conditions of biped model. The stability of the proposed controller to an unexpected disturbance should be considered. In this section, the stability of the proposed balance system is analyzed using the concept of Lyapunov exponents.

Chapter 2 proposed a neural approach to derive system Jacobians from RBFNN model for the calculation of Lyapunov exponents. This method can be used to analyze the stability of unknown systems. In this chapter, the biped balance system based on GA-based PD control is used to verify the effectiveness of the proposed neural method.

After an intensive training process of the RBFNN, all of the neural Jacobians are derived

from the RBFNN model using Equation (2.31) with the initial condition $[q_1, q_2, q_3, q_4]$= [-0.05*rad*, 0.03*rad*, 0.05*rad/s*, -0.03*rad/s*]. Figure 4.6 shows the neural Jacobians and the actual Jacobians deriving from the mathematic model. In the first rows of Figures 4.6(a)-4.6(p), the solid lines are the actual Jacobians $J_{ij} = \frac{\partial \dot{q}_i}{\partial q_j}$ ($i,j$=1,2,3,4) and the dashed lines are the neural Jacobians $\hat{J}_{ij} = \frac{\partial \hat{\dot{q}}_i}{\partial q_j}$ ($i,j$=1,2,3,4). The second rows in Figures 4.6(a)-4.6(p) show the absolute errors of these neural Jacobians. Since some elements of the Jacobians are zero, the absolute errors are presented.

After the biped stabilized in an upright posture, all of the elements of system Jacobians become constants, as the nonlinear terms of Equation (2.23) disappeared. The largest absolute error is less than 0.3. It is clear to see that the neural Jacobians are accurate in comparison with the actual Jacobians. The above results illustrate that the neural Jacobians can determine the actual Jacobians of the balance system successfully.

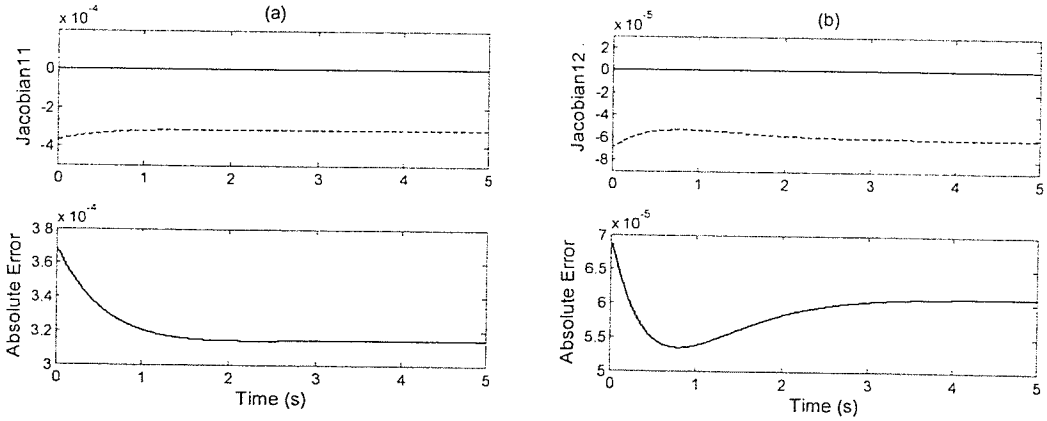

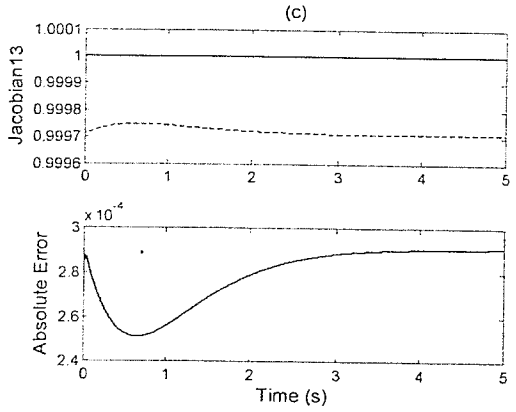
(c)
Jacobian13
1.0001
1
0.9999
0.9998
0.9997
0.9996
0 1 2 3 4 5
x 10^-4
Absolute Error
3
2.8
2.6
2.4
0 1 2 3 4 5
Time (s)

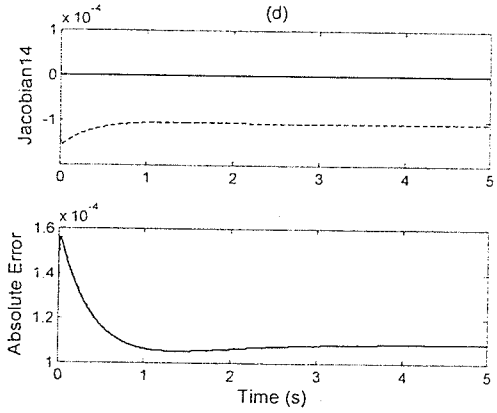
(d)
x 10^-4
Jacobian14
1
0
-1
0 1 2 3 4 5
x 10^-4
Absolute Error
1.6
1.4
1.2
1
0 1 2 3 4 5
Time (s)

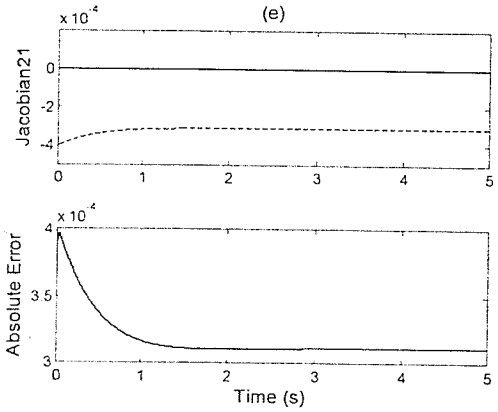
(e)
x 10^-4
Jacobian21
0
-2
-4
0 1 2 3 4 5
x 10^-4
Absolute Error
4
3.5
3
0 1 2 3 4 5
Time (s)

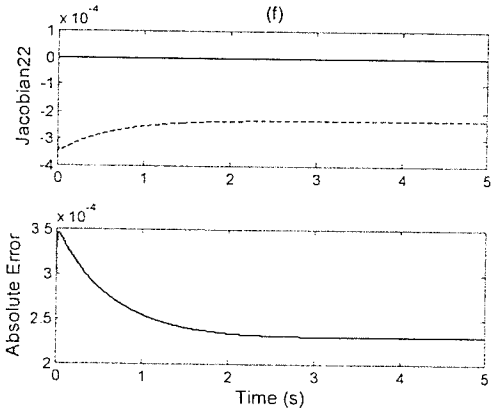
(f)
x 10^-4
Jacobian22
1
0
-1
-2
-3
-4
0 1 2 3 4 5
x 10^-4
Absolute Error
3.5
3
2.5
2
0 1 2 3 4 5
Time (s)

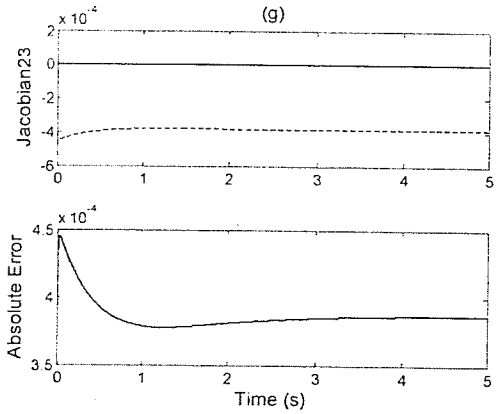
(g)
x 10^-4
Jacobian23
2
0
-2
-4
-6
0 1 2 3 4 5
x 10^-4
Absolute Error
4.5
4
3.5
0 1 2 3 4 5
Time (s)

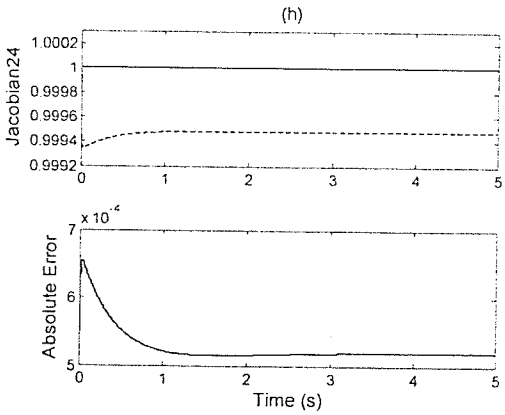
(h)
Jacobian24
1.0002
1
0.9998
0.9996
0.9994
0.9992
0 1 2 3 4 5
x 10^-4
Absolute Error
7
6
5
0 1 2 3 4 5
Time (s)

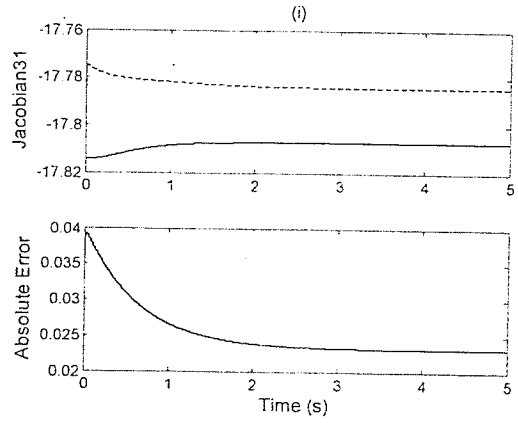
(i)
Jacobian31
-17.76
-17.78
-17.8
-17.82
Absolute Error
0.04
0.035
0.03
0.025
0.02
0 1 2 3 4 5
Time (s)

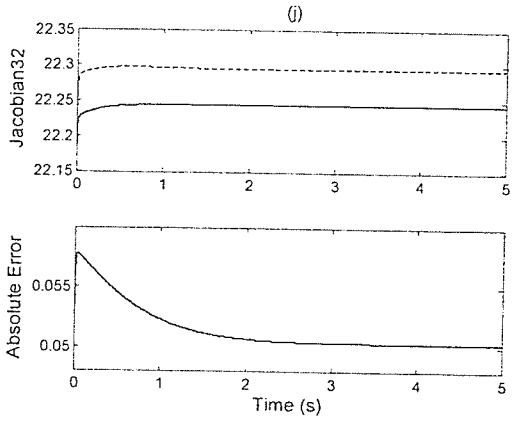
(j)
Jacobian32
22.35
22.3
22.25
22.2
22.15
Absolute Error
0.055
0.05
0 1 2 3 4 5
Time (s)

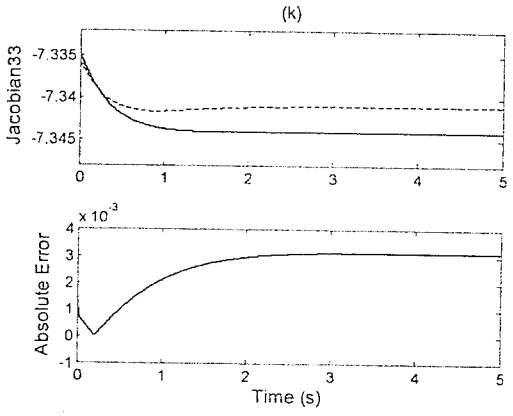
(k)
Jacobian33
-7.335
-7.34
-7.345
Absolute Error
x 10^-3
4
3
2
1
0
-1
0 1 2 3 4 5
Time (s)

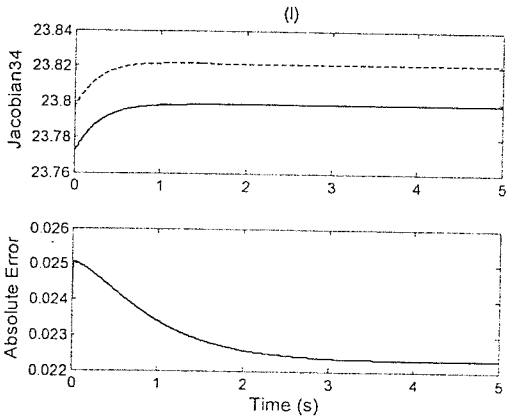
(l)
Jacobian34
23.84
23.82
23.8
23.78
23.76
Absolute Error
0.026
0.025
0.024
0.023
0.022
0 1 2 3 4 5
Time (s)

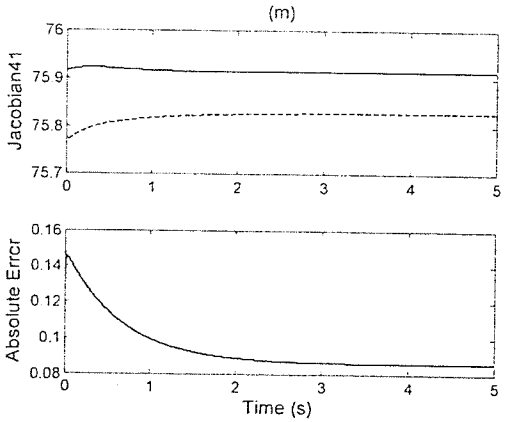
(m)
Jacobian41
76
75.9
75.8
75.7
Absolute Error
0.16
0.14
0.12
0.1
0.08
0 1 2 3 4 5
Time (s)

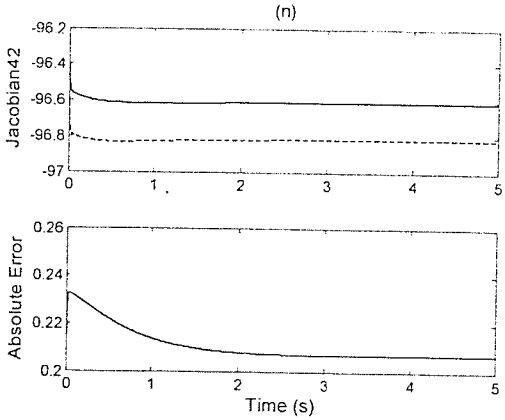
(n)
Jacobian42
-96.2
-96.4
-96.6
-96.8
-97
Absolute Error
0.26
0.24
0.22
0.2
0 1 2 3 4 5
Time (s)

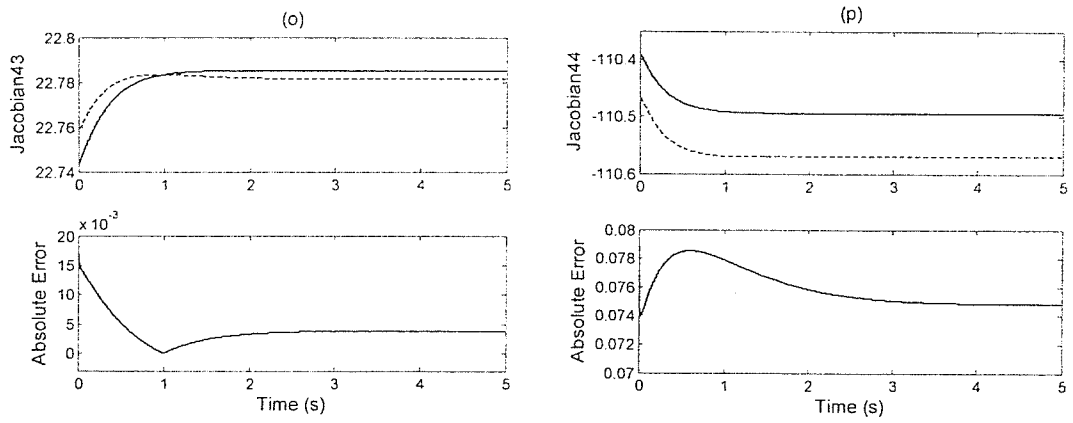


Figure 4.6 The actual and neural Jacobians of the GA-based PD control system: the actual Jacobians $J_{ij}$ (solid lines), the neural Jacobian $\hat{J}_{ij}$ ($i,j$=1,2,3,4)(dashed lines).

Four Lyapunov exponents are calculated. Figure 4.7 shows the four Lyapunov exponents in 100 seconds. The solid lines are the Lyapunov exponents based on the mathematical model. The dashed lines are the Lyapunov exponents, based on the neural model. The relative errors of the neural Lyapunov exponents are also shown in Figure 4.7. It is clear to see that the relative errors of the neural Lyapunov exponents are very low. The neural Lyapunov exponents are accurate in comparison with the actual ones.

It is demonstrated that the proposed approach to calculate Lyapunov exponents based on the RBFNN model is a constructive tool to analyze the stability of unknown systems. After 100 seconds, all of the Lyapunov exponents converge to negative constants (Table 4.1), which indicate the PD based GA control system is exponentially stable about the biped upright posture.

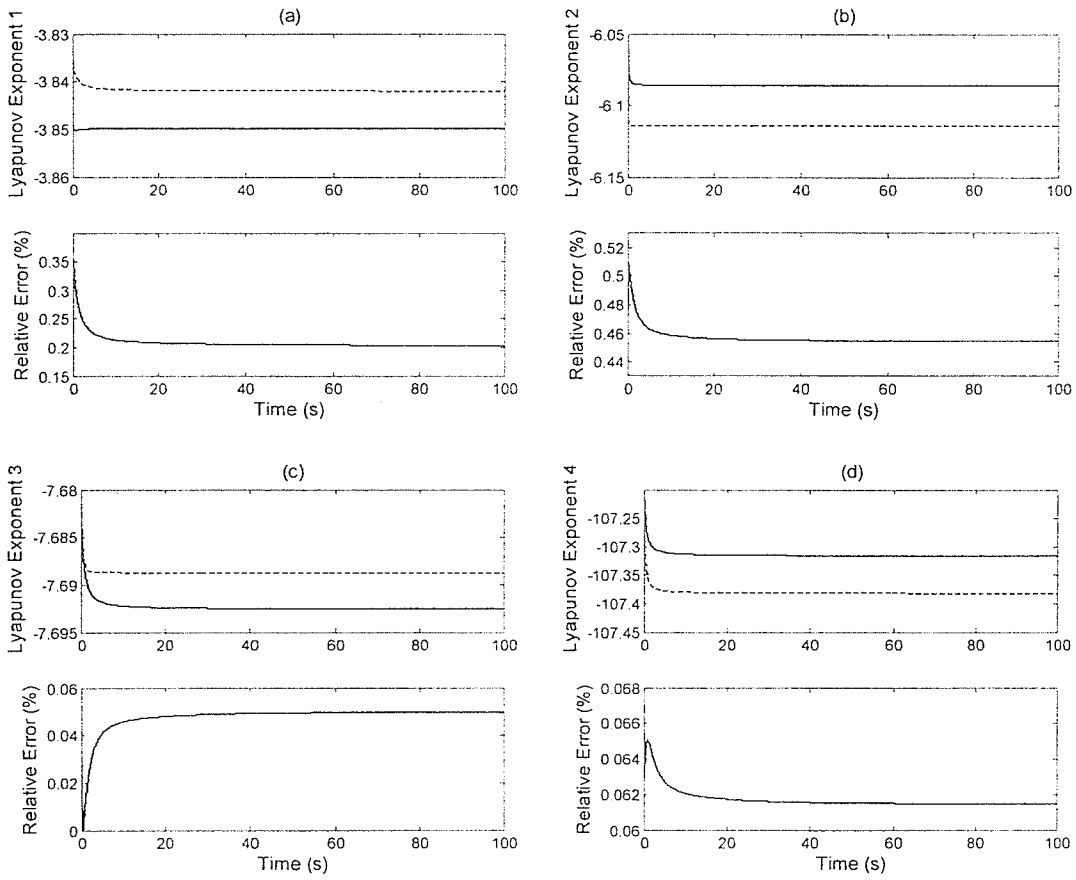


Figure 4.7 The Lyapunov exponents calculated based on the actual (solid lines) and neural models (dashed lines) of the GA-based PD control system: the (a) largest Lyapunov exponent (LE) (b) second LE (c) third LE (d) fourth LE.

| Lyapunov exponents (LEs) | 1st LE | 2nd LE | 3rd LE | 4th LE |
|---|---|---|---|---|
| Mathematical model | -3.8499 | -6.0860 | -7.6922 | -107.3131 |
| Neural model | -3.8417 | -6.1140 | -7.6887 | -107.3797 |
| Relative error | 0.213% | 0.460% | 0.046% | 0. 062% |

Table 4.1 The Lyapunov exponents and their relative errors after 100 seconds

The PD gains of the proposed controller are in respect to specific initial conditions. The results of Lyapunov exponents are different for each set of PD gains. Finding the entire

stability region for a specific set of PD gains is extremely difficult and it is out of the scope of this work.

The following is an example of part of the stability region of the PD gain ($K_{P1}$= 725.82, $K_{P2}$=236.21, $K_{D1}$= 171.75, and $K_{D2}$= 179.39). The regions:

$$\Gamma_1 = \{q_1 \in [-1.5,1.5]rad, q_2 \in [-1.5,1.5]rad, q_3 = 0rad/s, q_4 = 0rad/s\}$$

$$\Gamma_2 = \{q_1 \in [-1.5,1.5]rad, q_2 = 0rad, q_3 \in [-1.5,1.5]rad/s, q_4 = 0rad/s\}$$

$$\Gamma_3 = \{q_1 \in [-1.5,1.5]rad, q_2 = 0rad, q_3 = 0rad/s, q_4 \in [-1.5,1.5]rad/s\}$$

$$\Gamma_4 = \{q_1 = 0rad, q_2 \in [-1.5,1.5]rad, q_3 \in [-1.5,1.5]rad/s, q_4 = 0rad/s\}$$

$$\Gamma_5 = \{q_1 = 0rad, q_2 \in [-1.5,1.5]rad, q_3 = 0rad/s, q_4 \in [-1.5,1.5]rad/s\}$$

$$\Gamma_5 = \{q_1 = 0rad, q_2 = 0rad, q_3 \in [-1.5,1.5]rad/s, q_4 \in [-1.5,1.5]rad/s\} \quad (4.3)$$

in the phase plane, are divided into grid boxes with sizes of 0.01rad, 0.01rad, 0.01rad/s and 0.01rad/sec for $q_1, q_2, q_3$ and $q_4$, respectively. If the same convergent and negative largest exponent is obtained, the neighboring grid box belongs to the stability region.

The stability region (grey color) is shown in Figure 4.8. In the stability region all of the largest Lyapunov exponents are negative and the mean value is -3.8417 with a deviation of $4.21\times10^{-4}$.

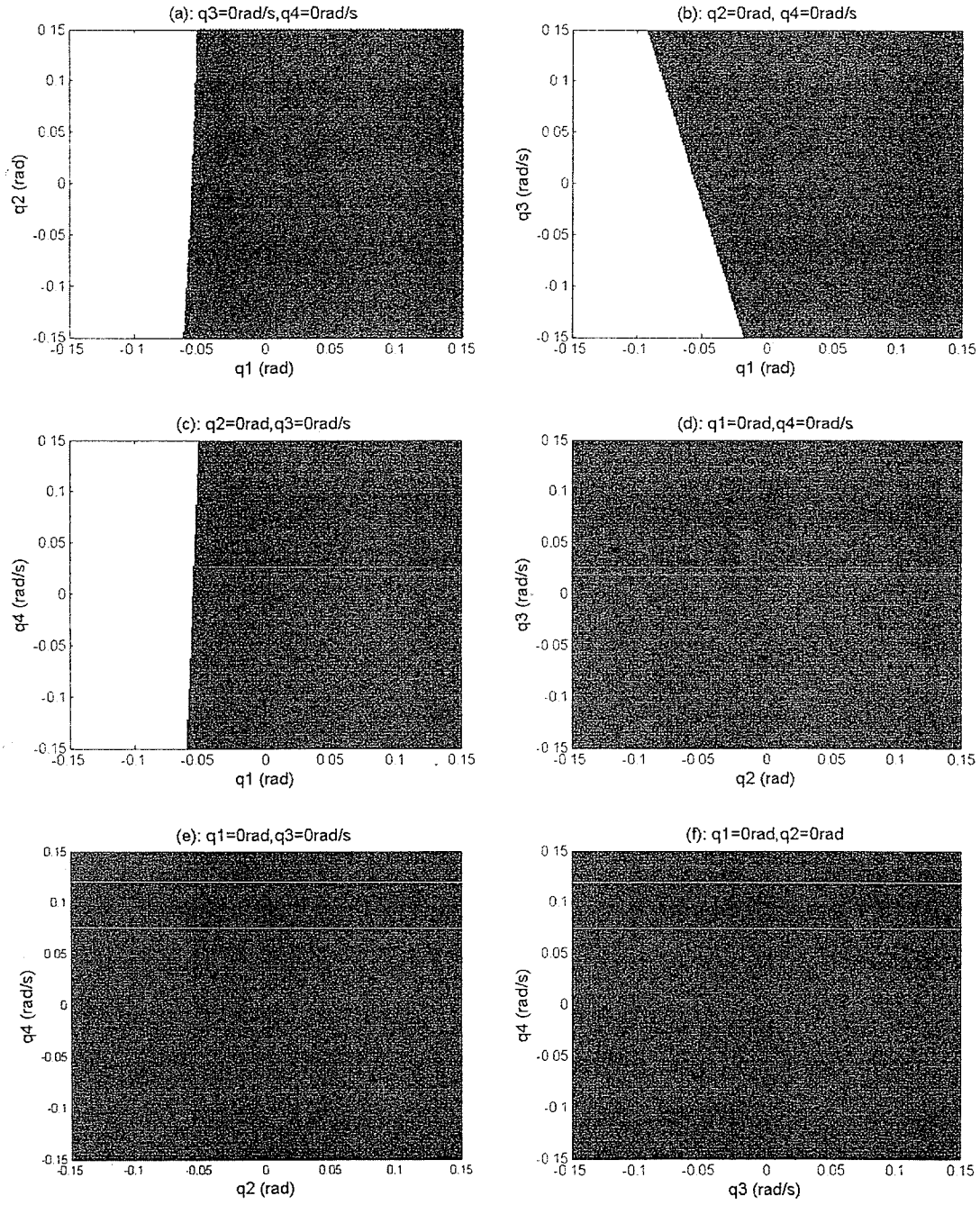


Figure 4.8 Part of the stability region of GA-based PD biped balance system

## 4.6 Discussion

Balance maintenance is a current research topic in the field of biped control. An important issue for biped control design is energy conservation. In my study, two optimal control schemes, derived from classical LQR techniques and GA techniques, have been proposed and implemented in the two-link biped model. In Chapter 3, the LQR balance control is designed to optimize the total energy consumption of torque outputs. In this chapter, a GA-based PD control is presented to keep the biped balance in the upright posture.

By using a GA as an optimization tool, it is easier to design an advance controller which can guarantee the satisfaction of the constraints between the feet and the ground as well as optimize the energy consumption of control outputs. With the above two balance systems implemented, the biped model is able to stay upright and balance during standing, and the total energy consumption of the torque outputs is low. In conclusion, both of two balance systems are successful in stabilizing the standing biped in the upright posture.

To evaluate the energy efficiency of the two controllers, the cost function in Equation (4.1) is employed. The values of the cost function $J$ are shown in Table 4.2, with some initial conditions. It is clear to see that the GA-based PD control has better performance for energy consumption in comparison to the LQR control.

| Initial condition (q1,q2,q3,q4) | LQR control | GA-based PD control |
|---|---|---|
| -0.02rad, 0.02rad, 0.05rad/s, -0.03rad/s | 0.0229 | 0.0217 |
| 0.15rad, 0.15rad, 0.01rad/s, 0.01rad/s | 11.37 | 11.01 |
| 0.05rad, 0.05rad, 0.01rad/s, -0.01rad/s | 1.272 | 1.204 |

Table 4.2 The values of the cost function using LQR control and GA-based PD control

The ability to keep the foot stationary is another important issue for biped control design. The limitation of the LQR control is that the gains are fixed. Since the primary aim of GA-based PD control is to guarantee the satisfaction of these foot constraints, the gains of this control method can be adapted according to initial conditions and the constraints between the foot-link and the ground. This means that in some cases, the LQR control fails but the GA-based PD control may not.

The following is an example with the initial condition ($q_1$=-0.045rad, $q_2$=0.045rad, $q_3$=0.001rad/s, $q_4$=-0.001rad/s). Figure 4.9(a) and (b) show the COP constraints of LQR control and GA-based PD control. The COP in the horizontal direction $x_{COP}$ , violates the lower bound at time $t$=0s, and the controller is terminated due to foot rotation. The GA-based PD controller successfully stabilizes the biped in an upright posture and the COP in the horizontal direction $x_{COP}$ is always within the bounds. It is concluded that the working region of GA-based PD control is larger than LQR control.

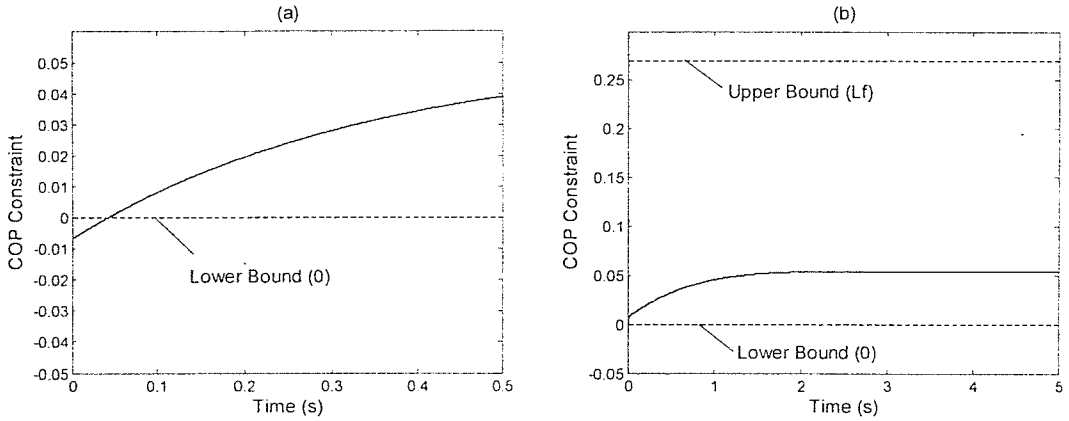


Figure 4.9 The COP constraint (a) LQR control (b) GA-based PD control

The stability of the GA-based PD control system is demonstrated by the concept of Lyapunov exponents and part of the stability region is determined. The method of calculating Lyapunov exponents based on RBFNN models is implemented on the GA-based PD control system. The results show that the neural method is accurate in comparison to the traditional method. Further, it demonstrates that the proposed method can be used to analyze the stability of complex or unknown systems without explicit knowledge of the mathematic models.

# Chapter 5

# Conclusions and Future Work

## 5.1 Conclusions

The overall goal of this thesis is two-fold: (1) to develop a control system that will keep the biped model in an upright posture despite adverse disturbances, and (2) to analyze the stability of the proposed control system using the concept of Lyapunov exponents.

The biped robot is simplified as two inverted pendulums, representing the legs and the trunk. The feet are modeled as a separate link stationary on level ground. The biped moves only in the sagittal plane. A dynamic model of the above biped robot and the inequalities resulted from the constraints between the foot-link and the ground, have been developed.

Two optimal controllers have been designed in this thesis. A LQR balance control is first designed to optimize the total energy consumption of torque outputs while keeping the biped in an upright position. The LQR problem is equivalent to a dynamic optimization problem for linear differential equations. It steers the solution of the underlying linear

differential equation to a desired reference trajectory with minimal cost, given the dynamic equations. Simulation results show that the LQR controller is effective for balance control with low control torques.

Although the satisfaction of the constraints between the foot-link and the ground was not considered in the control design, it has been closely examined in the computer simulations. It has been found that the low control torques have insignificant effects on the ground reaction forces. For example, the vertical ground reaction force is dominated by the gravity of the biped. The changes in the vertical ground reaction force are rather low. Similarly, the horizontal ground reaction force is lower than the maximum static friction, which indicates that the friction constraint can be easily satisfied. The simulations show that the COP constraint is easier to be violated due to the long leg and torso links and the short foot length. This finding is consistent with previous research (Yang and Wu, 2006a)

A GA-based PD balance control is then developed to keep the biped in an upright position, minimizing the energy consumption of torque outputs, and satisfying the constraints between the foot-link and the ground. The effectiveness of the control laws are tested through computer simulations, and the results show that all of the above three requirements are satisfied.

The stability of the biped control systems is the fundamental requirement for developing biped robots. In the current biped control field, an obstacle is the lack of an effective tool for stability analysis. In this work, the stability of the proposed balance systems is

analyzed using the concept of Lyapunov exponents. Part of the stability region has also been determined using Lyapunov exponents.

The Lyapunov exponents have been calculated using the mathematical model, for which the determination of the Jacobean matrices is crucial. Due to the complexity of the biped systems and even the unavailability of the mathematical model, the determination of Jacobeans is not always feasible. This prohibits the calculation of the Lyapunov exponents.

In this thesis, a new approach to calculate Lyapunov exponents based on a neural model is proposed to analyze the stability for complex or unknown systems. RBFNN is first employed for system identification and the Jacobians are derived from the neural model. Then, the Lyapunov exponents can be calculated using the above neural Jacobians.

For the biped systems with the above two optimal controllers, the Jacobians determined from the mathematical models and the corresponding neural models as well as the Lyapunov exponents from both the mathematical models and the neural models are compared, and they agree very well. For the Lyapunov exponents, the maximum relative errors are 0.6% and 0.5% for both control systems. RBFNN is used due to its outstanding characteristic of nonlinear system identification. This method is novel in that it is a framework, which makes the calculation of Lyapunov exponents feasible.

## 5.2 Future Work

The limitation of the proposed controllers is that the biped can be stabilized only in a static environment. Future work is to develop an advanced biped balance system using adaptive control and neural network control for an unknown dynamic environment. Stability analysis of such control schemes is still an open problem due to the complexity of the controller. Lyapunov exponents may be a good tool for this analysis. It should be noticed that the system Jacobians are variable, according to the environment and the learning algorithm. Analysis of the stability of such control law is another future development.

The proposed method to calculate Lyapunov exponents based on RBFNN model is a constructive tool to analyze the stability of unknown systems. However, the neural network should be retrained if the control law is changed.

In future work, control torques will be considered as input variables of system identification. We could find a general neural model of dynamic systems not dependent on controllers.

# References

Abarbanel, H.D.I.; Gilpin, M.E. and Rotenberg, M., *Analysis of Observed Chaotic Data*, Springer (New York), 1997.

Abdallah, M. and Goswami, A., "A biomechanical motivated two-phase strategy for biped upright balance control", *Proceedings of the 2005 IEEE International Conference on Robotics and Automation* 18(22), pp.1996-2001, 2005.

Al-Amoudi, A. and Zhang, L., "Application of radial basis function networks for solar-array modelling and maximum power-point prediction", *IEE Proceedings on Generation, Transmission and Distribution*, 147(5), pp. 310 – 316, 2000.

Arakawa, T. and Fukuda, T., "Natural motion trajectory generation of biped locomotion robot using Genetic Algorithm through energy optimization Systems", *IEEE International Conference on Man, and Cybernetics* 2, pp: 1495-1500, 1996.

Barbasin, E.A., "The construction of Lyapunov function for non-linear systems", *Proc. 1st International Congress of IFAC*, Moscow, pp. 943-947, 1960.

Bass, E. and Lee, K.Y., "A modified radial basis function network for system identification", *Proceedings of the 1994 IEEE International Symposium on Intelligent Control* 16-18, pp. 352-357, 1994.

Benetin, G.; Galgani, L.; Giorgilli, A. and Strelcyn, J.M., "Lyapunov characteristic exponents for smooth dynamical systems: a method for computing all of them. Part 1: Theory", *Meccanica* 15, pp. 9-20, 1980.

Broomhead, D.S. and Lowe, D., "Multivariable functional interpolation and adaptive networks", *Complex systems* (2), pp. 321-355, 1988.

Bors, A.G. and Gabbouj, G., "Minimal topology for a radial basis function neural network for pattern classification", *Digital Signal Processing: a review journal* 4(3), pp. 173-188, 1994.

Box, G. and Jenkins, G., *Time series analysis: forecasting and control*, Holden-Day, 1976.

Broomhead, D.S. and Lowe, D., "Multivariable functional interpolation and adaptive networks," *Complex system* 2, pp. 321-355, 1988.

Bykov, A.; Naumenko, O.V.; Pshenichnikov, A.M.; Sinitsa, L.N. and Scherbakov, A.P., "An expert system for identification of line in vibrational-rotational spectra", *Optics and Spectroscopy* 94(4), pp. 528-537, 2003.

Bryson J.A.E. and Ho, Y., *Applied optimal control*, Hemisphere, 1975

Caballero, M.A.R.; Armada, M. and Sanchez, V., "Extending zero moment point to a segment using reduced order biped model", *Climbing and Walking Robots (CLAWAR 2000) Professional Eng. Publishing (*London, UK*)*, 2000.

Cabodevial, G. and Abba, G., "Quasi optimal gait for a biped robot using genetic algorithm", *IEEE International Conference on Systems, Man, and Cybernetics* 4, pp. 3960-3965, 1997.

Capi, G.; Nasu, Y.; Barolli, L.; Yamano, M.; Mitobe K. and Takeda K., "A neural network implementation of biped robot optimal gait during walking generated by genetic algorithm", *The 9th Mediterranean Conf. Control and Automation* (Dubrovnik, Croatia), 2001.

Capi, G.; Nasu, Y.; Barolli, L.; Yamano, M. and Mitobe, K., "Real time gait generation for autonomous humanoid robots: A case study for walking", *Robotics and Autonomous Systems* 42(2), pp. 107-116, 2003.

Chin, P.S.M., "A genera method to derive Lyapunov function for Non-linear systems", *International Journal of Control* 44, pp. 381-393, 1986.

Chin, P.S.M., "Scalar-Lyapunov-function method for single and multi-machine problems in power system", *International Journal of Control* 45, pp. 1737-1749, 1987.

Chin, P.S.M., "Generalized integral method to derive Lyapunov functions for nonlinear systems", *International Journal of Control* 46, pp. 933-943, 1987.

Chin, P.S.M., "Stability results for the solutions of certain fourth-order autonomous differential equations", *International Journal of Control* 49, pp. 1163-1173, 1989.

Chen, S.; Cowan C.F.N. and Grant P.M., Orthogonal least squares learning algorithm for radial basis functions networks, *IEEE Trans. Neural Networks* 2(2), pp302-309, 1991.

Chen, S. and Billings, S.A., "Neural networks for nonlinear dynamic system modelling and identification", *International Journal Control* 56(2), pp 319-346, 1992.

Chew, C.M. and Pratt, G.A., "Adaptation to load variations of a planar biped: height control using robust adaptive control", *Robotics and Autonomous Systems* 35(1), pp.1-22, 2001.

Chow, C.K. and Jacobson, D.H., "Futher Studies of Human Locomotion: Postural Stability and Control", *Mathematical Biosciences* (15), pp. 93-108, 1972.

Cuevas, E.; Zaldívar D. and R. Rojas, "Incremental fuzzy control for a biped robot balance", *Proceeding Robotics and Applications* 498, 2005.

Dieci, L; Russell, R.D. and Van Vleck, E.S., "On the computation of Lyapunov Exponents for Continuous Dynamical Systems", *SIAM Journal of Numerical Analysis* 34(1), pp. 402-423, 1997.

Deng, R.; Davies, P. and Bajaj, A.K., "Flexible polyure-thane foam modeling identification of viscoelastic parameters for automotive seating applications", *Journal of Sound and Vibration* 262(3) pp. 391-417, 2003.

Duchon J, "Splines minimizing rotation-invariant semi-norms in Sobolev spaces, Constructive Theory of Functions of Several variables", *Lecture Notes in Mathematics* 38, pp. 85-100, 1977.

England, S.A. and Granata, K.P., "The influence of gait speed on local dynamic stability of walking", *Gait Posture* 25(2), pp.172-178, 2007.

Fang, Y. and Chow, T.W.S., "Orthogonal wavelet neural networks applying to identification of Wiener model", *IEEE Transactions on Circuits and Systems I: Fundamental Theory and Applications* 47(4), pp. 591-593, 2000.

Fukuda, T.; Komata, Y. and Arakawa, T., "Stabilization control of biped locomotion robot based learning with GAs having self-adaptive mutation and recurrent neural networks", *Proceedings of IEEE International Conference on Robotics and Automation* 1(20-25), pp.217 – 222, 1997.

Fukushima, H. and Sugie, T, "Model set identification in frequency-domain and its application to joint design with robust control", *Asian Journal of Control* 1(2), pp. 66-74, 1999.

Furusho, J. and Sano, A., "Sensor-Based Control of a Nine-Link Biped", *International Journal of Robotics Research* 9, pp. 83-98, 1990.

Garder, L.M. and Høvin, M.E., "Robot gaits evolved by combining genetic algorithms and binary hill climbing", *Proceedings of the 8th annual conference on Genetic and evolutionary computation* (Seattle, USA), pp: 1165-1170, 2006.

Gerth, W. and Albert, A. "New path planning algorithms for higher gait stability of a bipedal robot," *4th International Conference on Climbing and Walking robots* (Germany), 2001.

Goldberg, D.E., *Genetic algorithms in search, optimization, and machine learning*, Addison-Wesley, 1989.

Golliday, C.L. and Hemami, H., "Posture stability of the two-degree-of freedom biped by general linear feedback", *IEEE Transactions on Automatic Control* 21, pp. 74-79, 1976.

Golubovic, D. and Hu, H., "GA-based Gait Generation of Sony Quadruped Robots", *Proceedings of the 3rd IASTED International Conference Artificial Intelligence and Applications* (Benalmadena, Spain), 2003.

Gomm, J.B. and Yu, D.L., "Selecting radial basis function network centers with recursive orthogonal least squares training", *IEEE Transactions on Neural Networks*, 11(2), pp. 306-314, 2000.

Goodwin, G.C.; Graebe S.F. and Salgado M.E., *Control System Design*, Pearson US Imports & PHIPEs, 2000.

Gorinevski, D., "On the persistency of excitation in radial basis function network identification of nonlinear systems", *IEEE Transactions on Neural Networks* 6, pp. 1237-1244, 1996.

Goswami, A., "Foot rotation indicator (FRI) point: a new gait planning tool toevaluate postural stability of biped robots", *Proceedings of IEEE International Conference on Robotics and Automation* 1, pp.47-52, 1999.

Ghorbania, R.; Wu, Q. and Wang, G.G., "Nearly optimal neural network stabilization of bipedal standing using genetic algorithm", *Engineering Applications of Artificial Intelligence* 20(4), pp. 473-480, 2007.

Hardy, R.L., "Multiquadric equations of topography and other irregular surfaces", *Geophys. Res.* 76, pp. 1905-1915, 1971.

Hemami, H. and Golliday, C. Jr. "The inverted pendulum and biped stability", *Mathematical Bioscience* 34, pp. 95-110, 1977.

Hemami, H. and Cvetkovic, V.S., "Postural stability of two biped models via Lyapunov second method", *IEEE Transactions on Automatic Control* 22, pp. 66-70, 1977.

Hemami, H.; Barian, K., Jallics, L. and Heiss, D., "*Dynamics, stability, and control os stepping*", *Annuas of Biomechanical Engineering* 32(8), pp. 1153-1160, 2004.

Hemami, H.; Barian, K. and Pai, Y.C., "Quantitative analysis of the ankle strategy under translational platform disturbance", *IEEE Transactions on Neural Systems and Rehabilitation Engineering* 14(4), pp. 470-480, 2006.

Hemami, H. and Cvetkovic, V.S., "Postural stability of two biped models via Lyapunov second method", *IEEE Transactions on Automatic Control* 22, pp. 66-70, 1977.

Hemami, H. and Golliday, C.J., "The inverted pendulum and biped stability", *Mathematical bioscience* 34, pp. 95-110, 1977.

Hemami, H. and Utkin, V.I., "On the dynamics and Lyapunov stability of constrained and embedded rigid bodies", *International Journal of Control* 75(6), pp. 408-420, 2002.

Hemami, H. and Wyman, B.F., "Modeling and control of constrained dynamic systems with application to biped locomotion in the frontal plane", *IEEE Transactions on Automatic Control* 24, pp. 526-535, 1979.

Holland, H., *Adaptation in natural and artificial systems*, Univ. of Michigan Press, Reprinted in MIT Press, 1992.

Hu, J.; Pratt, J. and Pratt, G., "Stable adaptive control of bipedal walking; robot with CMAC neural networks", *Proceedings of IEEE International Conference on Robotics and Automation* 2, pp.1050-1056, 1999.

Huaux, A., "On the construction of Lyapunov function", *IEEE transactions on Automation and Control* 12, pp. 465, 1967.

Hurmuzlu, Y. and Moskowitz, G. D., "Bipedal locomotion stabilized by impact and switching: I. two- and three- dimensional, three-element models", *Dynamics and stability of system* 2, pp.75-96, 1987.

Hurmuzlu, Y., "Dynamics of bipedal gait: Part I – Objective functions and contact event of a planar five-link biped", *Journal of Applied Mechanics* 660, pp. 331-336, 1993.

Hurmuzlu, Y., "Dynamics of bipedal gait: Part II – Stability analysis of a planar five-link biped", *Journal of Applied Mechanics* 660, pp. 331-336, 1993.

Iqbal, K.; Hemami, H. and Simon, S., "Stability and control of a frontal four-link biped system", *IEEE Transactions on Biomechanical Engineering* 40(10), pp. 1007-1018, 1993.

Ito, S.; Takishita, H. and Sasaki, M., "A study of biped balance control using proportional feedback of ground reaction forces, *SICE-ICASE International Joint Conference* (Busan, Korea), 2006.

Jenkins, G. and Watts, D., "Spectral Analysis and Its Applications", Holden-day, 1968.

Jiang, Y.; Sachio, N. and Hidenori, K., "Dynamic model of body sway control during upright stance in human", *Japanese Journal of Physical Fitness and Sports Medicine* 55, pp.231-235, 2006.

Jiang, Y.; Sachio, N. and Hidenori, K., "A PID Model of Balance Keeping Control and Its Application to Stability Assessment", *2006 IEEE/RSJ International Conference on Intelligent Robots and Systems*, pp. 5925-5930, 2006.

Johnson, M.A. and Grimble, M.J., "Recent trends in linear optimal quadratic multivariable control system design", *IEE proc. Part D* 134(1), pp. 53-71, 1987.

Kadirkamanathan, V. and Niranjan, M., "A function estimation approach to sequential learning with neural networks", *Neural Computation* 5(6), pp. 954-975, 1993.

Kajita, S.; Kanehiro, F.; Kaneko, K.; Yokoi, K. and Hirukawa, H., "The 3D linear inverted pendulum mode: a simple modeling for a biped walking pattern generation", *Proceedings of IEEE/RSJ International Conference on Intelligent Robots and Systems* 1, pp.239-246, 2001.

Kalman, R.E., "Contributions to the theory of optimal control", *Bol. Soc. Mat. Mexicana* (5), pp. 102-119, 1960.

Kinsner, W., *Fractal and Chaos Engineering*, Lecture notes. Department of Electrical and Computer Engineering, University of Manitoba, 1996.

Krishnakumar, K. and Melkote, S.N., "Machining fixture layout optimization using the genetic algorithm", *International. Journal of Machine Tools & Manufacture* (40), pp. 579-598, 2000.

Kruglov, S.P.; Zalozhnev, A.Y. and Novikov, D.A., "Problem of center assignment in linear active systems", *Avtomatika I Telemekhanika* 12, pp. 78-91, 2002.

Kubica, E.; Wang, D. and Winter, D., "Feedforward and deterministic fuzzy control of balance and posture during human gait," *Proceedings 2001 ICRA. IEEE International Conference on Robotics and Automation* 3, 2001.

Kun, A. and Miller, W.T. III, "Adaptive dynamic balance of a biped robot using neural networks", *Proceedings of IEEE International Conference on Robotics and Automation* (Minneapolis, USA) 1, pp.240-245, 1996.

Kuo, A.D., "An optimal control model for analyzing human posture balance", *IEEE Trans. On biomedical engineering* 42, pp. 87-101, 1995.

Langari, R. and Wang, L., "A modified RBF network with application to system identification", *Proceedings of the 4th IEEE Conference on Control Applications*, (Albany, USA), pp. 649-654, 1995.

Lewis, F.L., *Optimal control*, Wiley, 1986.

Li, A.T.Q. and Kato, I., "Learning of walking stabilization for a biped robot with a trunk", *2nd Asian Conference on Robotics and Its Applications* (Beijing), 1994.

Liu, H.; Iberall, T. and Bekey, G.A., "Neural network architecture for robot hand control", *IEEE on Control Systems Magazine* 9(3), pp. 38-43, 1989.

Ljung, L., "System Identification: Theory For the User", Prentice-Hall, 1987.

Lyapunov, A.M., 1892, "The general problem of the stability of motion", Translated by Fuller, A.T., *International Journal of Control* 52, pp. 531-773; also (London: Taylor&Francis), 1992.

Yingwei, L.; Sundararajan, N. and Saratchandran, P., "Identification of time-varying nonlinear systems using minimalradial basis function neural networks", *IEE Proceedings of Control Theory and Applications* 144(2), pp. 202-208, 1997.

Ma, B. and Wu, Q., "Parametric study of repeatable gait for a planar five-link biped", *Robotica* 20, 493-498, 2002.

Marino, R. and Nicosia, S., "Hamiltonian-type Lyapunov functions", *IEEE Transactions on Automatic Control 28*, pp. 1055-1057, 1983.

Marmarelis, P. Z. and Marmarelis, V. Z., *Analysis of physiological systems: the white-noise approach*, Plenum Press, 1978.

Matej, S. and Lewitt, R.M., "Practical considerations for 3-d image reconstruction using spherically symmetric volume elements", *IEEE Transactions on medical imaging* (15), pp. 68 – 78, 1996.

Matzen, V.C. and McNiven, H.D., "Investigation of the inelastic characteristics of a single story steel structure using system identification and shaking table experiments", *Report No. EERC* 76-20, 1976.

Meng, Q. and Zhou, C., "Dynamic balance of a biped robot using fuzzy reinforcement learning agents", *Fuzzy set techniques for intelligent robotic systems (Fuzzy Sets and Systems)* 134(1), 2003.

Michalewich, Z., *Genetic Algorithms + Data Structures =Evaluation Programs*, Springer-Verlag, 1996.

Mikens, R.E., "Nonstandard finite difference schemes for differential equations", *Journal of Difference Equation and Applications* 8, pp. 823-847, 2002.

Mikens, R.E. and Gumel, A.B., "Construction and analysis of a nonstandard finite difference scheme for the bugers-fisher equation", *Journal of Sound and Vibration* 257, pp. 791-797, 2002.

Miura, H. and Shimoyama, I., "Dynamic walking of a biped locomotion", *International Journal of Robotics Research* 3, pp. 60-73, 1984.

Moody, J. and Darken, C. J., "Fast learning in network of locally-tuned processing units", *Neural Computation* 1, pp. 281-294., 1989.

Mu, X. and Wu, Q., "Development of a complete dynamic model of a planar five-link biped and sliding mode control its locomotion during the double support phase", *International journal of Control* 77, pp.789-799, 2004.

Müller, P.C., "Calculation of Lyapunov exponents for dynamic systems with discontinuities", *Chaos, Solitans and Fractals* 5, pp. 1671-1681, 1995.

Murray, M.P.; Seireg, A. and Scholz, R.C., "Center of gravity, center of pressure, and supportive forces during human activities", *J Appl Physiol* 23(6), pp. 831-838, 1967

Narendra, K.S. and Parthasarathy, K, "Identification and control of dynamical systems using neural networks", *IEEE Transactions on Neural Networks* 1(1), pp 4-27, 1990.

Niku, S.B., *Introduction to Robotics: Analysis, Systems, Applications*, Prentice Hall, 2001.

Nusse, H.E. and Yorke, J.A., *Dynamics: Numerical Explorations*, Springer, 1998

Oseledec, V.I., "A multiplicative ergodic theorem: Lyapunov characteristic numbers for dynamical systems", *Trans. Moscow Math. Soc.* 19, pp.197, 1968.

Paden, B.E. and Sastry, S.S., "A Calculus for computing Filippov's differential inclusion with application to the variable structure control of robot manipulators", *IEEE Transactions on Circuits and Systems* 34, 73-82, 1987.

Pai, Y.C. and Patton, J., "Center of Mass Velocity-Position Predictions for Balance Control", *Journal of Biomechanics* 30, pp. 347-354, 1997.

Park, J.H. and Choi, M., "Generation of an optimal gait trajectory for biped robots using a genetic algorithm", *JSME international Journal series C* 47(2), pp: 715-721, 2004.

Park, J.H. and Kim, K.D., "Biped robot walking using gravity-compensated inverted pendulum mode and computed torque control", *Proceedings of IEEE International Conference on Robotics and Automation* 4, pp. 3528-3533, 1998.

Park, J.H. and Rhee, Y.K., "ZMP trajectory generation for reduced trunk motions of biped robots", *Proceedings of IEEE/RSJ International Conference on Intelligent Robots and Systems* 1, pp. 90-95, 1998.

Parker, T.S. and Chua, L.O., "Practical numerical algorithms for chaotic systems", Springer Verlag (1989).

Platt, J., "A resource-allocating network for function interpolation", *Neural Computation* 3, pp.213-225, 1991.

Poggio, T. and Girosi, F., "Networks for approximation and learning", *Proceedings of the IEEE* 78, pp. 1481-1497, 1990.

Powell, J.D., "Radial basis functions for multivariable interpolation: A review", *Algorithms for approximation in Clarendon Press Institute of Mathematics And Its Applications Conference* (New York, USA), pp. 143-167, 1985.

Powell, J.D., "Radial basis function approximations to polynomials", *Pitman Research Notes in Mathematics Series, Numerical analysis*, pp. 223 – 241, 1987.

Ponzo, P.J., "On the stability of certain non-linear differential equations", *IEEE transactions on Automatic Control* 10, pp. 470, 1965.

Rank, E., "Application of Bayesian trained RBF networks to nonlinear time-series modeling", *Signal Processing* 83(7), pp. 1393-1410, 2003.

Sakai, M.; Homma, N; Yano, M. and Abe, K., "Lyapunov spectrum analysis of reconstructed attractors from observed time series", *SICE Annual Conference in Fukui*, 2003.

Sano, M. and Sawada, Y., "Measurement of the Lyapunov spectrum from chaotic time series", *Physic Review Letter* 55, pp. 1082, 1985.

Scesa, V.; Mohamed, B.; Henaff, P. and Ouezdou, F.B., "Dynamic recurrent neural network for biped robot equilibrium control: preliminary results", *ICRA Proceedings of the IEEE International Conference on Robotics and Automation* 18(22), pp.4114-4119, 2005.

Schagen, I. P., "Internal modeling of objective functions for global optimization", *Journal of Optimization Theory and Applications* 51(2), pp. 345-353, 1986.

Sanner, R.M. and Slotine, J.-J.E., "Gaussian networks for direct adaptive control", *IEEE Transactions on Neural Networks* 3(6), pp. 837-863, 1992

Sekhavat, P.; Sepehri, N. and Wu, Q., "Calculation of Lyapunov exponents using nonstandard finite difference discretization scheme: a case study", *Journal of difference equations and applications* 10(4), pp. 369-378, 2004.

Shevitz, D. and Paden, B., "Lyapunov stability theory of non-smooth systems", *IEEE Transactions on Automatic Control* 39, pp. 1910-1914, 1994.

Silva F.M. and Tenreiro Machado, J.A., "Energy analysis during biped walking", *Proceedings of IEEE International Conference on Robotics and Automation* 1, pp. 59-64, 1999.

Soderstrom, T. and Stoica, P., *System Identification*, Prentice Hall, 1987.

Southwood, S.C.; Radcliffe, C.J. and MacCluer, C.R., "Robust non-linear stick-slip friction compensation", *ASME Journal of Dynamic Systems, Measurement and Control* 113, pp. 639-644, 1990.

Sugihara, T.; Nakamura, Y. and Inoue, H., "Real-time Humanoid motion generation through ZMP manipulation based on the inverted pendulum control", *IEEE International Conference on Robotics & Automation* 2, pp. 1404 - 1409, 2002.

Thiffeault, J.L. and Boozer, A.H., "Geometrical constraints on finit-time Lyapunov exponents in two and three dimensions", *Chaos* 11, pp. 16-28, 2001

Scesa, V.; Mohamed, B.; Henaff, P. and Ouezdou, F.B., "Dynamic Recurrent Neural Network for Biped Robot Equilibrium Control: Preliminary Results", *Proceedings of the 2005 IEEE International Conference on Robotics and Automation*, pp: 4114- 4119, 2005.

Vukobratović, M.; Frank, A.A. and Juricic, D., "On the stability of anthropomorphic systems", *Mathematical Biosciences* 15, pp. 1-37, 1970.

Williams, G.P., *Chaos Theory Tamed*, Joseph Henry Press, Washington, D.C., 1997.

Wolf, A.; Swift, J.B.; Swinney, H.L. and Vastano, J.A. "Determining Lyapunov exponents from a time series", *Physica* 16D, pp. 285-317, 1985.

Wu, Q., "Lyapunov stability analysis of a class of base-excited inverted pendulums with application to bipedal locomotion systems", Ph.D. Thesis, University of Manitoba, 1996.

Wu, Q. and Chan, Y.A., "Design of energy efficient joint profiles for a planar five-link biped robot", *Proceedings of IEEE International Symposium on Computational Intelligence in Robotics and Automation*, pp. 35-40, 2001.

Wu, Q.; Sekhavat, P; Sepehri, N. and Peles, S., "On design of continuous Lyapunov's feedback control", *Journal of Franklin Institute, Engineering and Applied Mathematics* 342(6), pp. 702-723, 2005.

Wu, Q.; Thornton-Trump, A.B. and Sepehri, N., "Lyapunov stability control of inverted pendulums with general base point motion", *International Journal of Nonlinear Mechanics* 33, pp. 801-818, 1998a.

Wu, Q.; Onyshko, S.; Sepehri, N. and Thornton-Trump, A.B., "On construction of smooth Lyapunov functions for non-smooth systems", *International Journal of Control* 69, pp. 443-457, 1998b.

Wu, Q. and Sepehri, N., "On Lyapunov's stability analysis of non-smooth systems with applications to control engineering", *International Journal of Nonlinear Mechanics* 36, pp. 1153-1161, 2001.

Yamasaki, F.; Hosoda, K. and Asada M. "An energy consumption based Control for Humanoid Walking", *IEEE/RSJ IROS*, pp. 2473-2477, 2002.

Yang, C. and Wu, Q., "Effects of constraints on bipedal balance control", *Proceedings of the 2006 American Control Conference* (Minneapolis, USA)14(16), pp. 2510-2515, 2006a.

Yang, C. and Wu, Q., "On Stabilization of Bipedal Robots during Disturbed Standing Using the Concept of Lyapunov Exponents", *Robotica* 24(5), pp. 621-624, 2006b.

Yue, M and Schlueter, R., "Bifurcation subsystem identification", *IEEE on Power Engineering Society Summer Meeting* 3, pp.1599-1604, 2002.